Atmos. Meas. Tech., 6, 1747–1759, 2013
www.atmos-meas-tech.net/6/1747/2013/
doi:10.5194/amt-6-1747-2013

Atmospheric Measurement Techniques
Open Access

MODIS 3 km aerosol product: applications over land in an urban/suburban region

L. A. Munchak[1,2], R. C. Levy[1], S. Mattoo[1,2], L. A. Remer[3], B. N. Holben[1], J. S. Schafer[1], C. A. Hostetler[4], and R. A. Ferrare[4]

[1]Earth Science Division, NASA Goddard Space Flight Center, Greenbelt, MD 20771, USA
[2]Science Systems and Applications, Inc., Lanham, MD 20709, USA
[3]Joint Center for Earth Systems Technology (JCET), University of Maryland Baltimore County, Baltimore MD, 21228, USA
[4]NASA Langley Research Center, Hampton, VA 23681, USA

Correspondence to: L. A. Munchak (leigh.a.munchak@nasa.gov)

Received: 31 January 2013 – Published in Atmos. Meas. Tech. Discuss.: 14 February 2013
Revised: 14 June 2013 – Accepted: 17 June 2013 – Published: 23 July 2013

Abstract. MODerate resolution Imaging Spectroradiometer (MODIS) instruments aboard the Terra and Aqua satellites have provided a rich dataset of aerosol information at a 10 km spatial scale. Although originally intended for climate applications, the air quality community quickly became interested in using the MODIS aerosol data. However, 10 km resolution is not sufficient to resolve local scale aerosol features. With this in mind, MODIS Collection 6 includes a global aerosol product with a 3 km resolution. Here, we evaluate the 3 km product over the Baltimore–Washington D.C., USA, corridor during the summer of 2011 by comparing with spatially dense aerosol data measured by airborne High Spectral Resolution Lidar (HSRL) and a network of 44 sun photometers (SP) spaced approximately 10 km apart, collected as part of the DISCOVER-AQ field campaign. The HSRL instrument shows that AOD can vary by over 0.2 within a single 10 km MODIS pixel, meaning that higher resolution satellite retrievals may help to better characterize aerosol spatial distributions in this region. Different techniques for validating a high-resolution aerosol product against SP measurements are considered. Although the 10 km product is more statistically reliable than the 3 km product, the 3 km product still performs acceptably with nearly two-thirds of MODIS/SP collocations falling within an expected error envelope with high correlation ($R > 0.90$), although with a high bias of ~ 0.06. The 3 km product can better resolve aerosol gradients and retrieve closer to clouds and shorelines than the 10 km product, but tends to show more noise, especially in urban areas. This urban degradation is quantified using ancillary land cover data. Overall, we show that the MODIS 3 km product adds new information to the existing set of satellite derived aerosol products and validates well over the region, but due to noise and problems in urban areas, should be treated with some degree of caution.

1 Introduction

For over 12 yr, the MODerate resolution Imaging Spectroradiometer (MODIS) instruments, flying aboard the Terra and Aqua satellites, have been collecting data concerning the global distribution of climate related variables. Several of these variables describe aerosols, which have been shown to be one of the largest sources of uncertainty in the climate system (IPCC, 2007). MODIS provides a suite of information about aerosol properties, including aerosol optical depth (AOD) and aerosol sizing parameters, that have been used extensively for climate studies (e.g. Kaufman et al., 2002; Bellouin et al., 2005; Quaas et al., 2008). Currently, three algorithms are used operationally to provide products to the public – the dark target algorithm over land (Kaufman et al., 1997a; Levy et al., 2007b, 2010), the dark target algorithm over ocean (Tanré et al., 1997; Remer et al., 2005, 2008) and the deep blue algorithm over land (Hsu et al., 2004, 2006). All produce data at a 10 km nominal spatial scale, which is an appropriate scale for climate studies (Remer et al., 2013).

Soon after launch, it was realized that the retrieved aerosol parameters could be used as proxies for estimating surface

air quality conditions (e.g. Hutchison, 2003; Wang and Christopher, 2003; Chu et al., 2003; Engels-Cox et al., 2004; Hutchison et al., 2004). The MODIS instruments are particularly appealing for air quality applications because the broad (2330 km) swath of the instrument allows most global locations to be monitored on a nearly daily basis. However, the 10 km resolution of the MODIS aerosol products is insufficient to resolve small-scale aerosol features, including point sources in urban areas (C. C. Li et al., 2005) and small fire plumes (Lyapustin et al., 2011). Although several research techniques exist to retrieve aerosols at higher spatial scales (100 m to 1 km) from MODIS observations (e.g. Lyapustin et al., 2011; Li et al., 2012), these have not been produced globally in an operational environment.

In response to clear scientific needs for aerosol observations at a higher spatial resolution, MODIS Collection 6 will include a global aerosol product at nominal 3 km scale, in addition to the standard 10 km resolution. This 3 km product will include retrievals based on both dark target algorithms (land and ocean). Remer et al. (2013), describe the 3 km product in detail, and analyze a six-month test database to compare the performance of the 3 km and 10 km products on a global scale. The 3 km product can show more spatial detail than the 10 km product, but agrees less well with ground-based sun photometers on a global scale. However, the 3 km product may be better at characterizing aerosol distributions on local scales, and can only be tested through comparison with dense observations on a small spatial scale. We wish to examine the 3 km aerosol product on a regional scale to determine the additional information content that the higher resolution retrieval provides, and the possible degradation in data quality introduced by moving to a higher resolution.

In this work, we focus primarily on AOD, because it has been used for surface air quality applications (van Donkelaar et al., 2006) and can easily be compared with lidar and sun photometer data. Specifically, we can evaluate AOD products at both 10 km and 3 km resolutions by comparing with surface- and airborne-based AOD measurements collected during the DISCOVER-AQ field campaign conducted during the summer of 2011 over the Baltimore–Washington D.C. corridor of the United States. We first assess the similarities and differences in 10 km and 3 km MODIS AOD images, and evaluate whether the 3 km product provides information that is not captured by the 10 km product. We look critically at the best method to validate the higher resolution aerosol retrieval against sun photometer measurements, and validate the 10 km and 3 km products for the campaign duration. The ability of the MODIS product at both 10 km and 3 km resolutions to capture spatial variability in AOD is also addressed. Due to the limited validation data for the over ocean variables, we will only address the land variables in this study.

2 The MODIS 3 km land algorithm

The retrieval method of the global MODIS 3 km aerosol product is thoroughly detailed in Remer et al. (2013). For the sake of completeness, we will briefly describe the land algorithm here. The 3 km algorithm emerges from the "dark target" retrieval methodology (Kaufman et al., 1997a; Tanré et al., 1997; Remer et al., 2005; Levy et al., 2007b, 2013), based on the concept that in the visible wavelengths, aerosols are bright and vegetated surfaces tend to be dark. The spectral contrast between aerosols and the surface can be used to retrieve quantitative information about aerosol properties.

To increase signal-to-noise, the MODIS algorithm retrieves aerosol parameters at a lower spatial resolution than the nominal (at nadir) 500 m top of atmosphere (TOA) reflectance measurements. The algorithm creates N by N "retrieval boxes" of pixels, in order to filter out the subset that is not desirable for aerosol retrieval. Thus, the 10 km algorithm works with 20×20 pixel retrieval boxes (400 pixels), whereas the 3 km algorithm works with 6×6 pixel retrieval boxes (36 pixels). Remer et al. (2013) describes how pixels are masked for cloud (Martins et al., 2002), sediments in water (Li et al., 2003), snow and ice (R. Li et al., 2005) and surfaces that are too bright for retrieval. The remaining pixels are sorted by their 0.66 μm reflectance, and the brightest 50 % and darkest 20 % of the remaining pixels are discarded. This means that in the 10 km (3 km) algorithm, there are at most 120 pixels (11 pixels) remaining from which to do aerosol retrieval. The reflectances of these remaining pixels are averaged, resulting in a set of spectral reflectance values to drive the aerosol retrieval. These spectral reflectance values are further "corrected" for gas absorption (e.g. Levy et al., 2013).

The expected "quality" of the retrieval is determined by the number of pixels that remain after all masking and filtering. If at least 51 pixels remain (out of 120) for 10 km or 5 pixels remain (out of 11) for 3 km, the retrieval is initially expected to be of "high" quality. The 10 km retrieval will be attempted only if 12 pixels remain (out of 120), but it is expected to be of low quality. There is no corresponding low quality attempt for the 3 km retrieval (Remer et al., 2013).

The over land algorithm performs the retrieval by matching the observed TOA spectral reflectance with lookup tables of pre-computed TOA spectral reflectance. The largest uncertainty is in characterizing the contribution of the surface to the TOA reflectance, for which errors of 0.01 can lead to errors of 0.1 in retrieved AOD. Kaufman et al. (1997b) showed that the surface contribution in the 0.47 and 0.66 μm bands can be related to the surface contribution in the 2.1 μm shortwave-IR (SWIR) band. The assumed relationship between the visible and SWIR was refined by Levy et al. (2007b), and is used as a constraint in the aerosol retrieval. As described by Levy et al. (2007b), the current retrieval uses three channels (0.47 μm, 0.66 μm, and 2.1 μm) to determine both the amount of aerosol (total AOD) and the relative ratio of fine and coarse aerosol models. The selection of the

fine and coarse aerosol models are prescribed by season and location. The resulting primary retrieved aerosol parameters over land are total AOD at 0.55 μm, the fractional contribution of the fine-dominated aerosol type, the constrained surface reflectance, and fitting error (Levy et al., 2013). All of these assumptions (aerosol lookup tables, assumed surface reflectance relationship, and methodology of the inversion) are identical for both 10 km and 3 km retrievals (e.g. Levy et al., 2013; Remer et al., 2013).

Previously, the MODIS 10 km product has been thoroughly evaluated against sun photometers on global scales. The global expected error (EE) of the 10 km AOD at 0.55 μm product over land is $\pm 0.05 \pm 0.15$ AOD (Levy et al., 2010), and a testbed of 10 km data produced with the Collection 6 MODIS algorithm shows that, globally, 69 % of MODIS-Aqua land AOD retrievals fall within this range when collocated and compared to ground-based sun photometer measurements (Levy et al., 2013). Remer et al. (2013) has compared the same testbed of global 3 km AOD data with sun photometers and show that it tends to validate less well than the 10 km. Specifically, since only 63 % of global collocations fell within expected error over land, a new expected error of $\pm 0.05 \pm 0.20$ AOD has been established for the 3 km land product (Remer et al., 2013). Although a new 3 km EE has been established, we choose to continue to use the more stringent 10 km EE in this paper. Therefore, in this paper, when "EE" is referred to, the $\pm 0.05 \pm 0.15$ AOD definition is employed, unless otherwise stated.

3 Data sources

3.1 MODIS products

This analysis uses five minute time length sections of the MODIS orbits, termed "granules", collected between 20 June 2011 to 31 July 2011 from both the Aqua and Terra satellites. The granules were created outside of the MODIS operational framework using the finalized MODIS aerosol Collection 6 algorithm and Level 1B inputs. Therefore, small differences between these granules and the publicly released granules are not expected, but may exist. Additionally, the MODIS land surface cover product (MCD12Q1) is used to characterize surface type. The land cover product uses a trained algorithm to characterize land surface at a 500 m resolution using 5 different classification schemes (Freidl et al., 2010). In this work, we only consider the 17-class International Geosphere-Biosphere Programme (IGBP) system (Loveland and Belward, 1997). Data from both the Terra and Aqua satellites are included in both the training dataset and the product.

3.2 AERONET/DRAGON

The AErosol RObotic NETwork (AERONET) (Holben et al., 1998) has 5 permanent stations operating in the study region. These stations were supplemented with an additional 39 temporary stations, distributed in a roughly 10 km by 10 km grid, termed the Distributed Regional Aerosol Gridded Observation Networks (DRAGON). This network provided an unprecedented opportunity to validate satellite derived aerosol properties at a high spatial resolution. Each station is equipped with a Cimel sun photometer (SP) measuring at eight spectral bands between 340 nm and 1020 nm. AOD is calculated at 550 nm using a quadratic log-log fit (Eck et al., 1999). The AOD retrieval is expected to be accurate to within ± 0.015 (Eck et al., 1999; Schmid et al., 1999).

In this work, we use the level 1.5 AERONET/DRAGON SP data, which are cloud screened (Smirnov et al., 2000) but not quality controlled. However, comparisons between level 1.5 and level 2.0 AOD have a correlation of 0.99, a slope of 1 and no offset, and the level 1.5 data contains more measurements.

3.3 High Spectral Resolution LIDAR (HSRL)

The NASA Langley Research Center airborne HSRL instrument calculates aerosol optical depth at 532 nm using independent measurements of vertically resolved aerosol backscatter and extinction, and is therefore expected to be more accurate than a standard backscatter lidar, which typically requires additional data and/or assumptions to produce extinction profiles, and therefore AOD, from the backscatter (Hair et al., 2008). The NASA Langley King Air B200 airplane flew 25 flights with the HSRL instrument aboard on 13 days between 1 July 2011 and 29 July 2011.

4 Results

4.1 Case studies

Because much of the value of the 3 km resolution retrieval is better at resolving smaller scale aerosol features, we first look at two case studies from differing days in the DISCOVER-AQ study. Figure 1 shows the 10 km (panels a and c) and 3 km (panels b and d) resolution MODIS AOD at 0.55 μm observed by MODIS-Aqua on 21 July 2011 at 18:30 UTC. On this day, there is a strong AOD gradient, with a change from 0.15 to 0.45 AOD over ~ 50 km, and a local AOD enhancement reaching to over 0.75. HYSPLIT back trajectories, using winds from the NAM model at 12 km resolution, show that the lower AOD air mass originated in the Midwestern United States, while the higher AOD air mass was coming from southern Virginia and North Carolina, which had active biomass burning nearby, and also passed over more urbanized regions. The two MODIS products both resolve the AOD gradient, and, in general, show the same aerosol situation. Both products resolve the SP measured AOD maximum of 0.75, although the 3 km product shows more high AOD pixels which may or may not be noise. The 3 km product is able to retrieve closer to clouds, and therefore shows

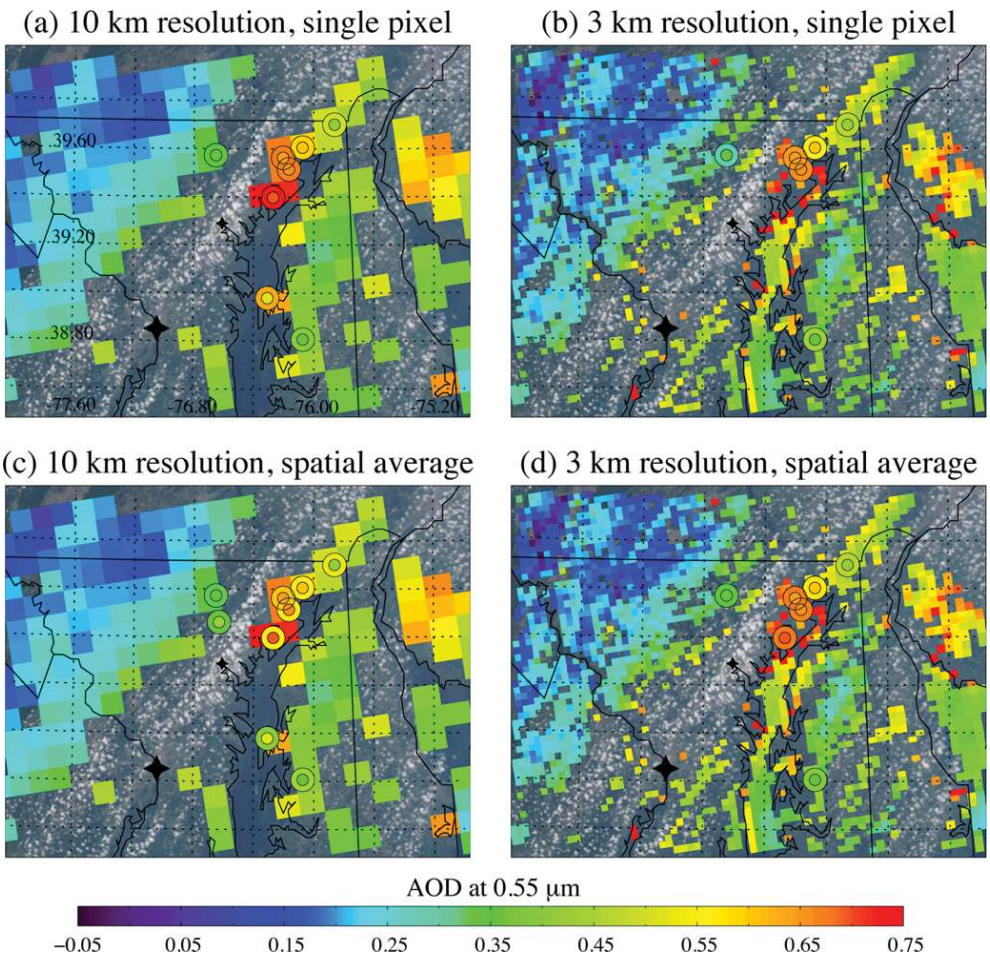

Fig. 1. AOD at 0.55 μm observed by MODIS-Aqua on 21 July 2011 at 18:30 UTC is plotted at the 10 km resolution (**a** and **c**) and 3 km resolution (**b** and **d**). MODIS/SP collocations are plotted in the circles. In **(a–d)**, the inner circle is the SP temporally averaged AOD, which is an average of ≥ 2 SP measurements within 30 min of MODIS overpass. In **(a)** and **(b)**, the outside circle is the AOD of the MODIS pixel containing the SP site. In **(c)** and **(d)**, the outer circle is the spatial average of a MODIS AOD in a 5×5 pixel box around the SP station. Only land pixels with a QA = 3 are used in the collocation. Washington D.C. is shown with the large black star and Baltimore, MD is shown with the small black star. The true color image, created from the MODIS red, green and blue bands, is shown in the background.

more detail and retrieves more area than the 10 km product. The 3 km product is also able to retrieve over bodies of water which are too narrow for 10 km retrievals, and has more pixels near the coastline that are unable to be retrieved by the 10 km product. The ability to retrieve closer to coastline is particularly valuable for air quality applications because many major cities, including some of the largest and most polluted, are located on coasts. This granule not only highlights the value of a high resolution satellite product, but also shows that AOD can vary significantly over small distances.

Plotted overtop of the MODIS AOD images in the circles are MODIS/SP collocations. In all of the panels (a–d), the inner circle shows the SP temporal mean, which is calculated by averaging all SP 0.55 μm AOD measurements at a station within 30 min of the MODIS overpass time, with a minimum of 2 observations. In the top row (panels a and b), the outer circle shows the 0.55 μm AOD of the MODIS pixel in which the SP station is located. In the bottom row (panels c and d), the outer circle shows the MODIS spatial mean, which is calculated by averaging all high quality (QA = 3) land pixels within a 5 pixel by 5 pixel box surrounding the SP station requiring at least 5 out of a possible 25 pixels (Ichoku et al., 2002). Therefore, the spatial averaging box for the 3 km product is 15 km by 15 km, and the spatial averaging box for the 10 km product is 50 km by 50 km. The single pixel MODIS collocations in the top row show excellent agreement between the MODIS retrieval and the SP measurements for both the 10 and 3 km products. However, the MODIS spatial average shown in the bottom row gives the impression that the 10 and 3 km products provide different answers; in this case, the smaller averaging box creates better MODIS/SP agreement for the 3 km product, while the larger averaging box of the 10 km product smoothes out the gradient and causes disagreement. The spatial averaging technique

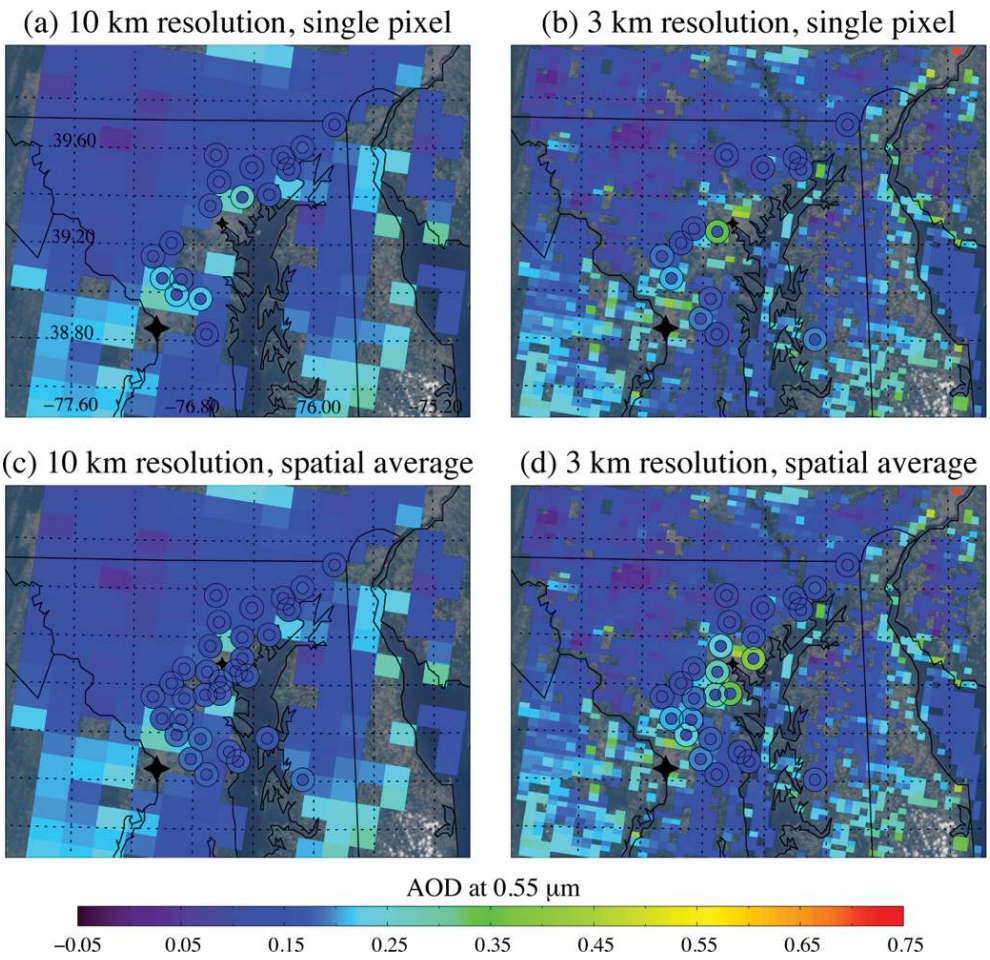

Fig. 2. AOD at 0.55 μm observed by MODIS-Terra on 1 July 2011 at 15:35 UTC is plotted at the 10 km resolution (**a** and **c**) and 3 km resolution (**b** and **d**). MODIS/SP collocations are plotted in the circles. In **(a–d)**, the inner circle is the SP temporally averaged AOD, which is average of ≥ 2 SP measurements within 30 min of MODIS overpass. In **(a)** and **(b)**, the outside circle is the AOD of the MODIS pixel containing the SP site. In **(c)** and **(d)**, the outer circle is the spatial average of a MODIS AOD in a 5 × 5 pixel box around the SP station. Only land pixels with a QA = 3 are used in the collocation. Washington D.C. is shown with the large black star and Baltimore, MD is shown with the small black star. The true color image, created from the MODIS red, green and blue bands, is shown in the background.

does increase the number of MODIS-SP collocations as compared to the single pixel technique, adding an extra collocation for each product. This granule shows that the single pixel collocation technique better characterizes AOD at the SP site, but limits the number of collocations and therefore the statistical robustness of the validation.

Figure 2 shows the 10 km and 3 km resolution MODIS AOD observed by MODIS-Terra on 1 July 2011 at 15:35 UTC, which has a markedly different aerosol distribution than that shown in Fig. 1. On this day, AOD is low (0.12 as measured by the SPs) and is homogeneous across the region. As in Fig. 1, the large-scale view of the two MODIS products agree, but there are nuanced differences. Some noisy pixels are present in the 3 km product, and are less apparent in the 10 km product. Both the 10 km and 3 km products have elevated AOD along the New Jersey and Delaware coastline, which are plausibly cloud contaminated from subpixel clouds. The 10 km has fewer contaminated pixels, but they extend further from the coastline; the 3 km product has more contaminated pixels, but their spatial extent is limited to right along the coastline. The 3 km product also shows a small amount of striping that results from differences in the MODIS instrument detectors. As in Fig. 1, the 3 km product has more coverage over the water areas in this scene. The MODIS/SP collocation circles are as they were in Fig. 1, with MODIS single pixel collocations shown in the outer circles of the top row, MODIS spatial average collocations in the outer circles of the bottom row, and SP temporal averages in the inner circle of all panels.

In this aerosol situation, the spatial averaging of the 10 km product AOD increases the agreement with the SP measurements because the averaging decreases the impact of noisy pixels. Twenty-eight out of the 31 collocations shown in Fig. 2c fall within expected error, and the average retrieved

0.55 μm AOD at the SP stations is 0.15, only 0.03 higher than the SP determined AOD. The MODIS 3 km spatially averaged collocations show an AOD enhancement of 0.1 to 0.3 over Baltimore City that is not observed by the SP measurements; 9 out of the 26 MODIS 3 km spatial averages shown in Fig. 2d have an above expected error. The largest difference between the MODIS 3 km and SP measurements was observed at the sun photometer station in Essex, Maryland, 13 km east of downtown Baltimore, where the SP AOD is 0.11, and the AOD of the 3 km spatial average is 0.38. A similar AOD enhancement is seen over Washington D.C., although there are no SP measurements to confirm that this enhancement is a retrieval artifact. The single MODIS pixel collocations in the Fig. 2b do not capture this important retrieval problem due to the coincidences of where the SP stations happen to be located and if the exact pixel where the station is located is retrieved. This case study suggests that the spatial average collocation technique better characterizes the retrieval performance over the larger region, and the single pixel collocation technique may misrepresent product performance because it is much more sensitive to the siting of the SP stations.

The airborne HSRL measurements provide an opportunity to look at aerosol extinction and AOD spatial variability with a nominal 1 min resolution, which corresponds to a nearly 6 km horizontal resolution. Figure 3 shows another high aerosol loading day, observed by MODIS-Terra on 29 July 2011 at 16:00 UTC. HSRL 532 nm columnar AOD along the flight track between 15:30 and 16:30 UTC is shown in the thick line, plotted atop of the 3 km resolution 0.55 μm AOD. The sections of the flight track where the plane was flying lower than 7 km, flying above clouds, or was turning are shown in grey. SP AOD interpolated to 0.55 μm is shown in the circles. The SP measurements are not temporally averaged; the nearest measurement to 16:00 UTC is used, provided the measurement was taken between 15:30 and 16:30 UTC.

The SP AOD measurements range from 0.33 to 0.58, with lower values towards the south and west, and higher values towards the north and east. The HSRL AOD measurements have a wider range from 0.35 to 0.67. There is excellent agreement between HSRL and SP measurements at the AERONET stations, which indicates that the broader range of AOD values from HSRL is likely due to the HSRL instrument being able to measure a larger area than the sun photometers and not due to inaccuracies in either measurement. The MODIS 3 km product generally captures the spatial pattern of AOD as observed by both the HSRL instrument and the sun photometers, although as in Fig. 2, the AOD is overestimated in the urban areas and there are noisy retrievals. Outside of the urban areas, the MODIS image shows AOD near 0.45 for much of the southern and western portion of the granule, increasing to 0.65–0.75 in the northeastern portion of the granule that also has HSRL and SP measurements.

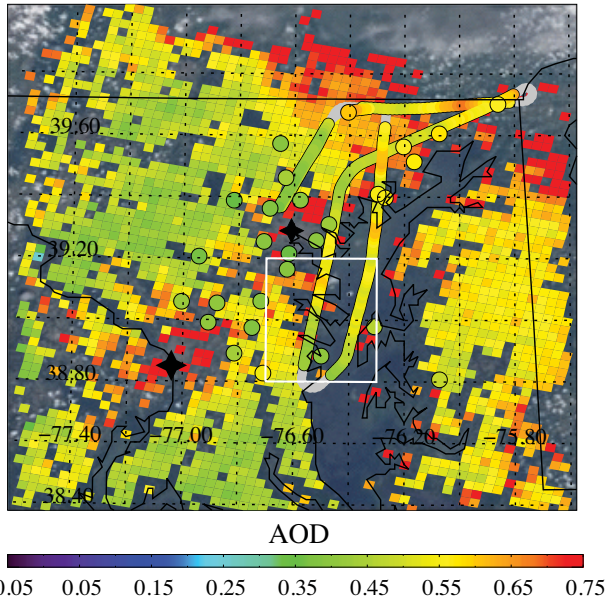

Fig. 3. A 3 km resolution AOD at 0.55 μm observed by MODIS-Terra on 29 July 2011 at 16:00 UTC is plotted in the background. HSRL 532 nm columnar AOD along the flight track between 15:30 and 16:30 UTC is shown in the thick line. SP AOD interpolated to 0.55 μm is shown in the circles. The SP measurements are not temporally averaged; the nearest measurement to 16:00 UTC is shown, provided the measurement was taken between 15:30 and 16:30 UTC. Washington D.C. is shown with the large black star and Baltimore, MD is shown with the small black star. The true color image, created from the MODIS red, green and blue bands, is shown in the background.

Overall, the three instruments show a similar aerosol situation albeit with varying levels of detail.

The HSRL AOD measurements reflect the more general pattern observed by the sun photometers, but also show many small-scale enhancements that cannot be observed even with the high spatial density of the DRAGON network. The western portion of the flight track in Fig. 4 shows that the HSRL instrument measured an increase in AOD from 0.41 to 0.59 over ∼ 4 min between 16:00:08 and 16:04:28 UTC, and traveling south by 29.8 km and west by 5.3 km in this time period. This change takes place over three 10 km boxes and ten 3 km boxes. The MODIS 3 km product better retrieves the absolute change in AOD, although the gradient along the flight track is not well reproduced because of missing and noisy pixels. The maximum AOD is overestimated in the 10 km product, and is more accurately retrieved in the 3 km product, although a neighboring pixel has an anomalously high AOD. It is probable that there is a source of contamination in the noisy 3 km pixel, which was included in the 10 km pixel along with the good pixels, resulting in an overestimation in the 10 km pixel. From this comparison, it is clear that while the 3 km product contains more noisy pixels that are likely contaminated, the smaller pixel size limits the spatial extent

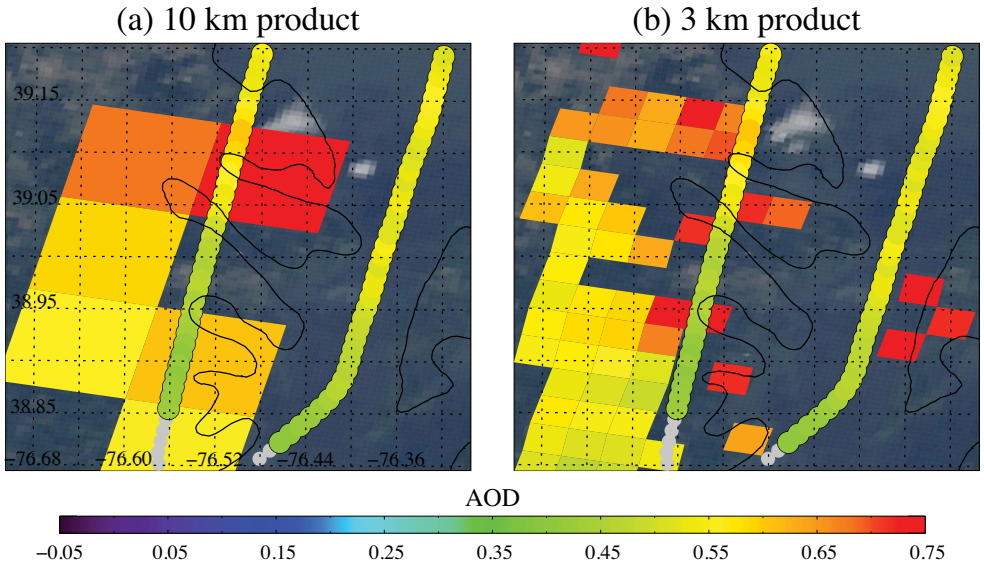

Fig. 4. Close up view of the area enclosed in the white box in Fig. 3. **(a)** MODIS 10 km 0.55 μm AOD with 532 nm HSRL AOD plotted on top. **(b)** MODIS 3 km 0.55 μm AOD with 532 nm HSRL AOD plotted on top.

of the contamination and allows nearby uncontaminated pixels to retrieve the correct AOD. In the 3 km product, the effects of cloud or surface contamination are larger within a single pixel, but at the same time are also spatially limited.

As highlighted in Fig. 4, because the HSRL instrument makes several measurements within a single MODIS pixel, it provides an opportunity to assess AOD variability across the standard MODIS retrieval resolution. A measure of subpixel AOD variability is shown in Fig. 5. For each 10 km resolution MODIS pixel, the minimum HSRL measured AOD is subtracted from the maximum HSRL AOD, provided the measurements are within half an hour of the MODIS overpass. Data from all flights that have valid data within half an hour of a MODIS overpass are included, and only MODIS pixels that contain more than 5 HSRL observations are analyzed to ensure that two fully independent HSRL measurements are obtained within the MODIS pixel. In all, 482 MODIS pixels are available for analysis for subpixel AOD variations. Within a single MODIS 10 km pixel, the maximum HSRL measured AOD change is 0.25, increasing from 0.36 to 0.61 AOD. The mean 0.55 μm AOD variation within a 10 km pixel is 0.037 while the median variation within a 10 km pixel is 0.023. Fewer than 25 % of pixels contained less than 0.01 AOD variation. The 10 km retrieval assumes uniformity of the AOD across the retrieval box, and that is simply not the case. The assumption is likely to hold better across the 3 km retrieval box; however, the nominal resolution of the HSRL instrument for this study is larger than the 3 km retrieval box. For this case, decreasing the HSRL nominal horizontal resolution for AOD from 6 km to 1 km increased the noise to an unacceptably high level such that

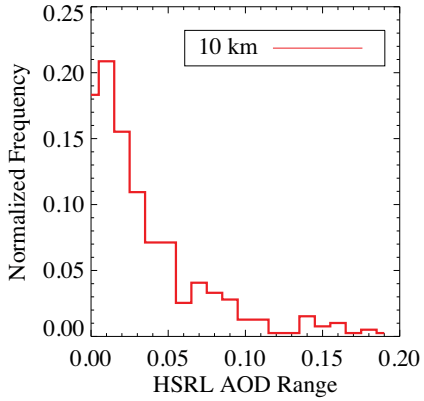

Fig. 5. The maximum difference between HSRL 0.55 μm AOD measurements observed within a MODIS 10 km pixel, normalized by the total number of analyzed grid boxes. Only MODIS pixels that contain 6 or more HSRL measurements are included.

the AOD variation within the MODIS 3 km pixels could not be quantified.

The case study comparisons with ground- and airborne-based AOD measurements show that the MODIS 3 km product contains additional aerosol information as compared to the 10 km product. Figure 1 shows a situation in which a few high AOD pixels in the 10 km product could be interpreted as noise, but the higher resolution of the 3 km product provides many more pixels, and SP data confirms that a true high aerosol loading event was identified. Additionally, the 3 km retrieval is able to retrieve over small bodies of water and close to coastline. The subpixel AOD variability observed by HSRL suggests that a 10 km product will frequently miss

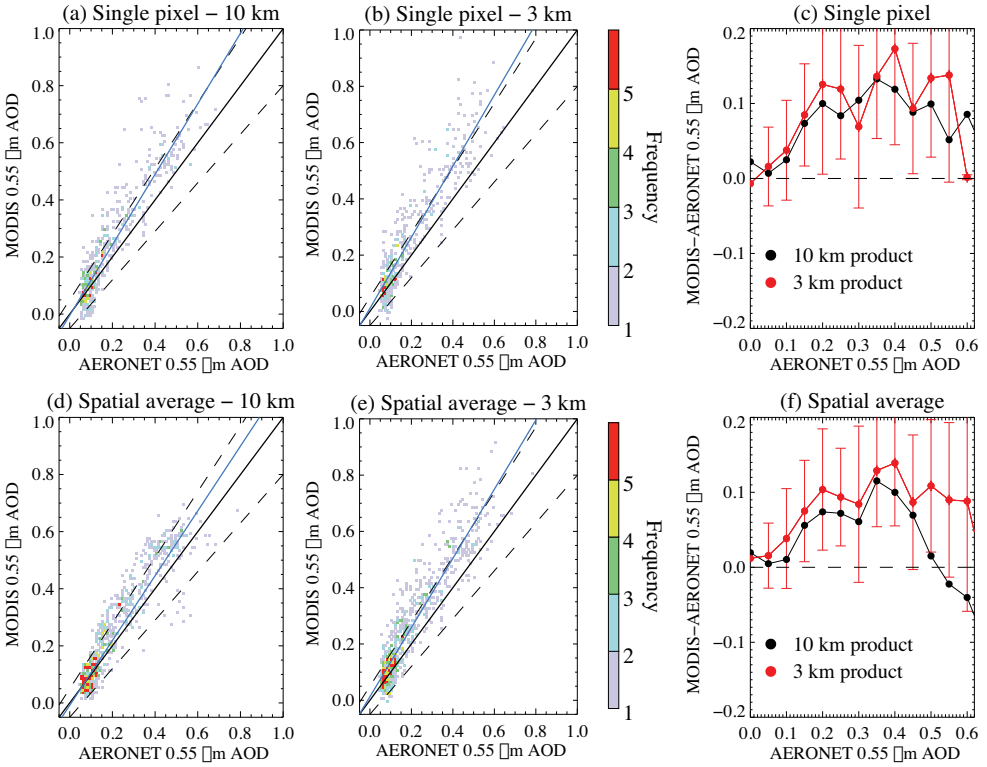

Fig. 6. (a) Density scatter plot of MODIS/SP collocations for 10 km AOD at 0.55 μm, using the single pixel collocation technique. Expected error over land (±0.05 ± 0.15 AOD) is shown in the dashed lines, the best fit line is shown by the solid blue line, and the one-to-one line is shown in the solid black line. **(b)** Same as in **(a)**, except for the 3 km product. **(c)** Average difference between MODIS single pixel collocations and SP 0.55 μm AOD, as a function of SP 0.55 μm AOD. A standard deviation of ±1 is shown for the 3 km product. **(d–f)** As in **(a–c)**, except the MODIS 5 × 5 pixel spatial average collocation is used.

small changes in AOD over an urban/suburban region. However, retrieving with a higher resolution reduces the statistical robustness of the aerosol product, resulting in more noise and inaccurate retrievals over urban areas.

4.2 MODIS 3 km validation

The case studies highlight the strengths and weaknesses of the 3 km product; however, the sun photometer data from the entire campaign provides the most comprehensive dataset to characterize its performance. The SP data also allows a critical look at how the different collocation techniques demonstrated in Figs. 1 and 2 lead to different conclusions on the validity on the MODIS AOD data in this region for both the 10 and 3 km resolutions.

In Fig. 6a, all 10 km MODIS/SP 0.55 μm AOD collocations are shown in a density scatter plot, using the MODIS single pixel collocation technique employed in Figs. 1a and 2a, and the same is shown in Fig. 6b for the 3 km product. In Fig. 6c, these single pixel MODIS/SP collocations are binned by the SP AOD, and the mean MODIS-SP difference for the bin is plotted for both the 10 and 3 km products. This process is repeated in Fig. 6d–f except that the 5 × 5 pixel MODIS spatial collocation technique is employed in the MODIS/SP collocations. The collocation statistics for both techniques for both products is shown in Table 1.

For both MODIS/SP collocation techniques, the bulk of the 3 km MODIS retrievals are within the ±0.05 ± 0.15 AOD expected error (63.6 % for the single pixel technique and 68 % for the spatial average technique). The satellite retrieval is highly correlated with the ground-based measurements, although with a small negative offset (0.011 for the single pixel technique and 0.013 for the spatial average technique) and a significant slope (1.26 for single pixel, 1.22 for spatial average). Accordingly, the MODIS 3 km AOD agrees well with SP AOD at low aerosol loadings, but is generally biased high at higher AOD. The primary difference between the two collocation techniques is that the spatial average has nearly twice as many collocations (817 as opposed to 451, for the 3 km product); therefore, the spatial averaging technique may be more representative of the region at large.

The binned MODIS-SP differences in Fig. 6c and f agree well with the impression given by the scatter plots. The bias of the MODIS 3 km product is near zero at AOD below 0.1, then is biased high above 0.1. The single pixel collocation is likely to best compare the 10 km and 3 km products, because the spatial averaging technique samples a different area for

Table 1. Statistics from the 4 different MODIS/SP collocations shown in Fig. 6a,b and d–e. N = number of valid collocations, R = correlation coefficient, Slope = slope of regression line (shown in blue in Fig. 6), Offset = y intercept of the regression line, bias = MODIS average AOD minus SP average AOD, RMSE = root mean square error of collocations. EE for all cases is $\pm 0.05 \pm 0.15$ AOD.

Product resolution	Averaging method	N	R	Slope	Offset	Bias	RMSE	% above EE	% within EE	% below EE
10 km	single pixel	499	0.925	1.235	0.004	0.049	0.093	26.7	69.3	4.0
10 km	spatial average	848	0.935	1.134	0.008	0.039	0.075	21.5	75.9	2.6
3 km	single pixel	451	0.914	1.263	0.011	0.062	0.109	33.7	63.6	2.7
3 km	spatial average	817	0.928	1.228	0.013	0.057	0.096	30.7	68.0	1.3

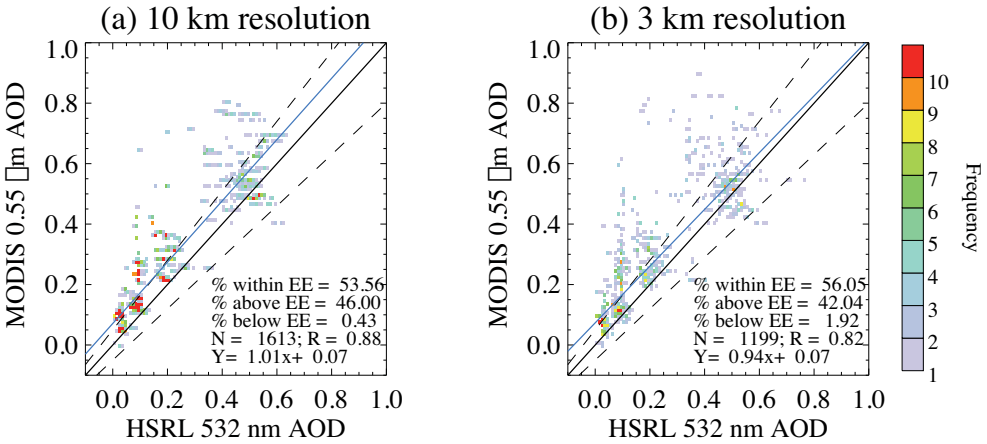

Fig. 7. Density scatter plot of MODIS/HSRL collocations for AOD at 0.55 μm for MODIS and 532 nm for HSRL for the 10 km MODIS product **(a)** and the 3 km MODIS product **(b)**. The MODIS AOD is sampled along the HSRL flight path; no spatial or temporal averaging is performed. Expected error over land ($\pm 0.05 \pm 0.15$ AOD) is shown in the dashed lines, the best fit line is shown by the solid blue line, and the one-to-one line is shown in the solid black line.

the different products. The 3 km product single pixel averages shown in Fig. 6c show that the average AOD of the 3 km product is frequently, but not always, higher than the 10 km product.

The retrieved AOD from the HSRL airborne instrument provides a different perspective on validation of the 3 km product. Because the plane is moving quickly in space, no spatial or temporal averaging is used to make the MODIS/HSRL collocations. The MODIS data are sampled along the HSRL flight track, provided that the HSRL observation is made within the geographic region mapped in Figs. 1 and 2, and is within 30 min of the MODIS overpass. Shortening the time requirement to either 15 or 5 min does not significantly affect the collocation statistics, but provides far fewer collocations. The HSRL and MODIS AOD are not interpolated to the same wavelength, which is expected to introduce between 2–4 % error (Kittaka et al., 2011). It is expected that the AOD retrieved by the HSRL instrument would be lower than the AOD retrieved by MODIS by at least 0.01 to 0.02 because the HSRL instrument does not measure the entire column, and therefore neglects the contribution of above the HSRL profile (i.e. above 7 km) to total columnar AOD.

Figure 7 shows that the both products agree with HSRL, but with significant high bias (0.093 for 10 km, 0.086 for 3 km). The increased bias of the 10 km product could be due to the pixel contamination effect shown in Fig. 4 – although the 3 km product contains more contaminated pixels, the spatial extent of those pixels is limited, allowing more correct pixels as well. The 10 km MODIS/HSRL comparison also shows the necessity of a higher resolution retrieval; the stripes in the HSRL/MODIS comparison show the change in HSRL AOD within a single pixel; the pattern that is quantified in Fig. 5.

From both SP and HSRL comparisons, we consider the 3 km product to be validated in this region. Using either collocation technique, more than 63 % of MODIS/SP collocations are within the expected error of the 10 km product, which is more stringent than the defined EE of the 3 km product. If the more lax $\pm 0.05 \pm 0.20$ AOD expected error definition for the 3 km product (Remer et al., 2013) is employed, then the percent of collocations within EE increases to 67.1 % for the single pixel collocation technique, and 73.1 % for the spatial collocation technique. However, the increased noise and urban problems give the 3 km product a larger high bias than the 10 km product as compared to SP

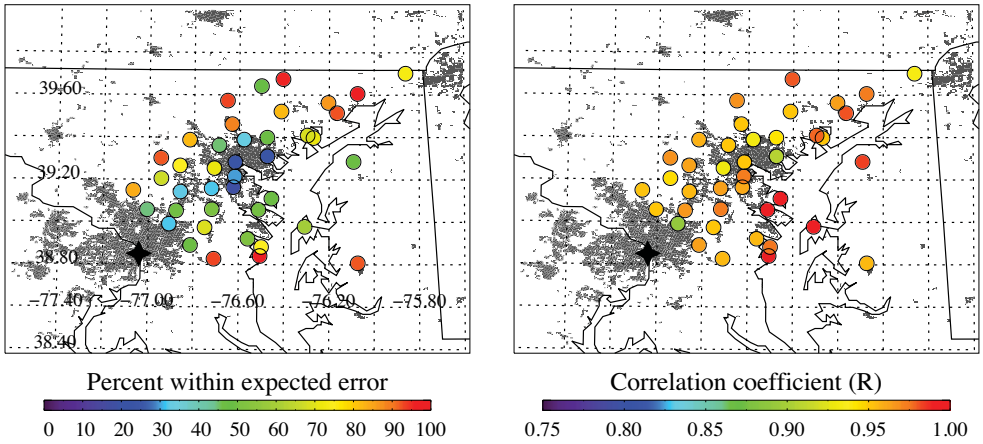

Fig. 8. (a) Percent of 3 km spatially averaged MODIS/SP collocations of 0.55 μm AOD within expected error (±0.05 ± 0.15 AOD) at each SP station. **(b)** Correlation coefficient between 3 km spatially averaged MODIS 0.55 μm AOD and SP temporally averaged 0.55 μm measurements at each station. Land identified as urban/built up by the MODIS land cover product (MCD12Q1) is plotted in grey in both panels.

measurements. The single pixel and spatial average MODIS collocation techniques show quantitative but not qualitative differences.

4.3 Sources of uncertainty

Figures 2 and 3 show an overestimation of AOD in urban areas. In order to study this further, we separate the 3 km MODIS/SP spatially averaged collocations by SP station, and compute agreement statistics for each station. We choose the spatial averaging collocation technique because it provides more collocations. The percent of comparisons within expected error for each station is shown in Fig. 8a, and the correlation coefficient (R) between MODIS and SP 0.55 μm AOD is shown in Fig. 8b. In each panel, land classified as "urban" by the MODIS Land Cover type product (MCD12Q1) is plotted in grey.

Figure 8a shows remarkable variability in the percent of collocations within EE for each SP station, ranging between 16 % to 95 %. The stations with the smallest percent within EE are clustered around the Baltimore urban center, and the more urbanized I-95 corridor between Washington D.C. and Baltimore. However, the stations with small percentages of collocations within EE still have correlation coefficients above 0.85, suggesting that the error is a systematic bias that could be accounted for in future retrievals, and not a random error.

We wish to quantify the urban overestimation of the 3 km product using the dense spatial distribution of the sun photometer sites in the DRAGON network. Using the same 15 km averaging box as the MODIS spatial collocation, the percent of pixels within the averaging box identified as urban by the MCD12Q1 product is calculated. In Fig. 9, this quantity is plotted against the percent of collocations above EE for each SP site. The percent of urban land within the MODIS averaging box is well correlated with the percent

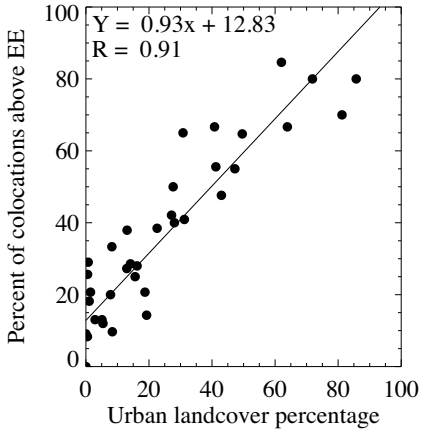

Fig. 9. Percent of 3 km spatially averaged MODIS/SP 0.55 μm AOD collocations above expected error (+0.05 + 0.15 AOD) at each SP station, plotted against the percentage of pixels within the 15 km by 15 km collocation box identified as urban by the MODIS land cover product.

of MODIS/SP collocations that are above the expected error. This confirms that the largest source of uncertainty in this study is related to the urban areas. The cause is suspected to be improper land surface reflectance characterization, considering that aerosol sources are not expected to vary significantly within the region of study and that it has been shown that the surface reflectance in the 0.66 μm channel over some urban surfaces is ∼ 0.7 of the 2.13 reflectance (Castanho et al., 2008; Oo et al., 2010) which is higher than the ratio used in the MODIS operational retrievals. In mixed-use urban/suburban regions like the DISCOVER-AQ study region, it is likely that the brighter urban surface 500 m pixels were selectively discarded in the pixel selection process of the 10 km product. However, because the resolution of the 3 km retrieval is smaller, more urban pixels remain within

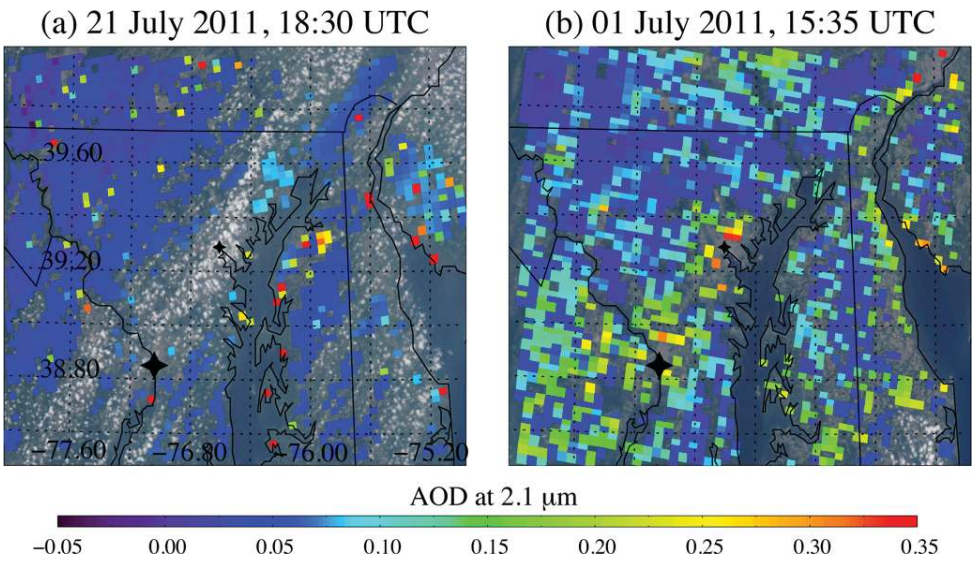

Fig. 10. (a) 3 km AOD at 2.1 μm observed by MODIS-Aqua on 21 July 2011 at 18:30 UTC. **(b)** 3 km AOD at 2.1 μm observed by MODIS-Terra on 1 July 2011 at 15:35 UTC. Only land pixels with a QA = 3 are shown. Washington D.C. is shown with the large black star and Baltimore is shown with the small black star. The true color image, created from the MODIS red, green and blue bands, is shown in the background.

the retrieval box after pixel selection, causing the surface reflectance in the visible wavelengths to be underestimated, leading to an overestimation in AOD.

Ideally, the noisy pixels could be flagged as poor quality, and therefore treated with some degree of caution. One of the products produced operationally is the AOD at 2.1 μm. This is not a validated product, but is used as a diagnostic to the retrieval. It may hold information that can identify poorer quality 3 km retrievals. In Fig. 10a, the 2.1 μm AOD on 21 July 2011 at 18:30 from the 3 km product is plotted, the same granule as that shown in Fig. 1b, and in Fig. 10b; the 2.1 μm AOD on 1 July 2011 at 15:35 UTC from the 3 km product is plotted, the same granule as that shown in Fig. 2b. The scene-wide 2.1 μm AOD is 0.046 in the left panel, and is 0.065 in the right panel. Both granules contain pixels with a 2.1 μm AOD over 0.2, more than 3 to 5 times higher than the scene-wide average. The error is not due to the wrong aerosol model being picked; in both scenes, all of the pixels were assigned the fine mode dominated urban aerosol model (Levy et al., 2007a). It appears that the same pixels that have anomalously high 2.1 μm AOD retrievals also tend to have inaccurate 0.55 μm AOD retrievals. For example, the pixels with high (> 0.55) AOD in Fig. 1b that agree with SP observations have retrieved 2.1 μm AOD values that do not stand out from the background. However, the pixels with high AOD in Fig. 2b that do not agree with SP observations have retrieved 2.1 μm AOD values significantly higher than the background. Although the 2.1 μm AOD retrieval is an unvalidated product, it may serve a purpose as a consistency check in this fine mode dominated, urban environment. This consistency check is likely to be inapplicable in dusty or other coarse mode dominated regimes.

Using anomalous 2.1 μm AOD pixels as a proxy for poor quality 0.55 μm pixels, and therefore throwing them out, results in a reduction of the both the negative bias at low AOD and the positive bias at high AOD. If the 3 km product is filtered such that pixels with a 2.1 μm AOD over 0.2 are excluded, and MODIS/SP are collocated using the spatial averaging technique, the percent within EE rises from 68 % to 78 %, while the number of collocations falls from 817 to 727, and the R rises from 0.92 to 0.95. However, this screening is not globally applicable, and is not recommended for use without closer examination.

It appears that a primary source of error in the 3 km MODIS aerosol product is the incorrect estimation of surface reflectance over urban regions. This error is not as apparent in the 10 km product because brighter urban surfaces are preferentially discarded during the pixel selection process. However, because the 3 km product has a smaller footprint, it is likely that not all urban pixels are discarded, and the surface reflectance is underestimated, leading to an overestimation in AOD. The 2.1 μm AOD shows some potential as an imperfect filter for these poor quality pixels.

5 Summary and conclusions

The MODIS dark target aerosol algorithms were designed with climate applications in mind, and the spatial scale of the retrieval reflects that design. However, as the applications of the aerosol product have evolved, the proper scale at which to observe small-scale aerosol events came into question. In response to the needs for aerosol observations at a higher resolution than 10 km, an operational aerosol product

produced at a 3 km resolution will be available in MODIS Collection 6.

This new product was evaluated against ground and airborne data over the Baltimore–Washington D.C., USA corridor over the summer of 2011 to understand the potential added information from the higher resolution retrieval and the statistical reliability of the product. The 10 km and 3 km granules generally resolve similar large scale patterns in aerosol distribution but differ in the details. The smaller footprint of the 3 km product retrieves closer to clouds and over small bodies of water, but also makes the product more susceptible to cloud contamination and other sources of noise. Subpixel comparisons against HSRL show that AOD can vary significantly within a 10 km pixel, and a 3 km resolution is a more appropriate scale for studying aerosol distributions in urban and suburban settings.

The dense network of sun photometers deployed during the DISCOVER-AQ campaign provided an unprecedented opportunity to validate aerosol products at a high spatial scale. Given the new resolution of both the satellite data and the ground validation network, the MODIS spatial-temporal collocation techniques for validation were revisited. It was found that using a spatial average of MODIS pixels around a sun photometer station, or using only the pixel where the SP station is located resulted in a quantitative, but not qualitative, difference. We conclude with good confidence that the MODIS 3 km validates in this region, but is biased high at AOD values greater than 0.1.

There is evidence that a significant source of the bias observed in the 3 km product results from improper characterization of urban surfaces. The method for attributing the surface contributions to TOA measured reflectances has been documented to underestimate the surface reflectances in urban areas (Castanho et al., 2008; Oo et al., 2010), which in turn overestimates AOD. Indeed, we found a strong correlation between the amount of urban surface near a sun photometer station, and the percent of collocations that are above the expected error. While case studies show that the 10 km product also has one or two pixels that are affected, the smaller pixel size of the 3 km product causes it to be more susceptible to contamination.

The poor performance of the 3 km product over urban surfaces is clearly a limitation in terms of air quality applications. How to best address this problem in an operational environment remains an open question. However, despite this limitation, the 3 km aerosol product has new capabilities for studying aerosol on local scales, including resolving small scale AOD gradients and point sources, retrieving aerosol in patchy cloud fields, and retrieving closer to coastlines. We expect that the added information of the 3 km resolution product will complement the existing MODIS 10 km resolution aerosol product and products from other passive and active sensors to provide a more complete view of global aerosol properties from space.

Acknowledgements. The authors thank Bill Ridgway and the MODAPS team for facilitating iterative testing needs. We also thank the University of Wisconsin PEATE team for the production of the Terra L1B data used in previous iterations of this study. We recognize the entire AERONET team for their efforts to deploy and maintain 44 functioning AERONET stations. HSRL operations were funded by the NASA DISCOVER-AQ program. The authors also thank the NASA Langley King Air flight crew for their outstanding work supporting these flights.

Edited by: M. King

References

Bellouin, N., Boucher, O., Haywood, J., and Reddy, M. S.: Global estimate of aerosol direct radiative forcing from satellite measurements, Nature, 438, 1138–1141, 2005.

Castanho, A. D., Martins, J. V., and Artaxo, P.: MODIS Aerosol Optical Depth Retrievals with high spatial resolution over an Urban Area using the Critical Reflectance, J. Geophys. Res., 113, D02201, doi:10.1029/2007JD008751, 2008.

Chu, D. A.: Global monitoring of air pollution over land from the Earth Observing System-Terra Moderate Resolution Imaging Spectroradiometer (MODIS), J. Geophys. Res., 108, 4661, doi:10.1029/2002JD003179, 2003.

Eck, T. F., Holben, B. N., Reid, J. S., Dubovik, O., Smirnov, A., O'Neill, N. T., Slutsker, I., and Kinne, S.: Wavelength dependence of the optical depth of biomass burning, urban and desert dust aerosols, J. Geophys. Res., 104, 31333–31350, 1999.

Engel-Cox, J. A., Holloman, C. H., Coutant, B. W., and Hoff, R. M.: Qualitative and quantitative evaluation of MODIS satellite sensor data for regional and urban scale air quality, Atmos. Environ., 38, 2495–2509, 2004.

Friedl, M. A., Sulla-Menashe, D., Tan, B., Schneider, A., Ramankutty, N., Sibley, A., and Huang, X.: MODIS Collection 5 global land cover: Algorithm refinements and characterization of new datasets, Remote Sens. Environ., 114, 168–182, 2010.

Hair, J. W., Hostetler, C. A., Cook, A. L., Harper, D. B., Ferrare, R. A., Mack, T. L., Welch, W., Izquierdo, L. R., and Hovis, F. E.: Airborne high spectral resolution LIDAR for profiling aerosol optical properties, Appl. Optics, 47, 6734–6752, 2008.

Hutchison, K. D.: Applications of MODIS satellite data and products for monitoring air quality in the state of Texas, Atmos. Environ., 37, 2403–2412, 2003.

Hutchison, K. D., Smith, S., and Faruqui, S.: The use of MODIS data and aerosol products for air quality prediction, Atmos. Environ., 38, 5057–5070, 2004.

Holben, B. N., Eck, T. F., Slutsker, I., Tanre, D., Buis, J. P., Setzer, A., Vermote, E., Reagan, J. A., Kaufman, Y. J., Nakajima, T., Lavenu, F., Janowiak, I., and Smirnov, A.: AERONET – A federated instrument network and data archive for aerosol characterization, Remote Sens. Environ., 66, 1–16, 1998.

Hsu, N. C., Tsay, S. C., King, M. D., and Herman, J. R.: Aerosol Properties Over Bright-Reflecting Source Regions, Ieee T. Geosci. Remote, 42, 557–569, 2004.

Hsu, N. C., Tsay, S. C., King, M. D., and Herman, J. R.: Deep blue retrievals of Asian aerosol properties during ACE-Asia, IEEE T. Geosci. Remote, 44, 3180–3195, 2006.

Ichoku, C., Chu, D. A., Mattoo, S., Kaufman, Y. J., Remer, L. A., Tanré, D., Slutsker, I., and Holben, B. N.: A spatio-temporal approach for global validation and analysis of MODIS aerosol products, Geophys. Res. Lett., 29, MOD1.1–MOD1.4, doi:10.1029/2001GL013206, 2002.

IPCC1: AR4 WG, Climate Change 2007: The Physical Science Basis, Contribution of Working Group I to the Fourth Assessment Report of the Intergovernmental Panel on Climate Change, edited by: Solomon, S., Qin, D., Manning, M., Chen, Z., Marquis, M., Averyt, K. B., Tignor, M., and Miller, H. L., Cambridge University Press, ISBN 978-0-521-88009-1, 2007.

Kaufman, Y. J., Tanré, D., Remer, L., Vermote, E., Chu, A., and Holben, B.: Operational remote sensing of tropospheric aerosol over land from EOS moderate resolution imaging spectroradiometer, J. Geophys. Res., 102, 17051–17067, 1997a.

Kaufman, Y. J., Wald, A., Remer, L., Gao, B., Li, R., and Flynn, L.: The MODIS 2.1 μm channel – Correlation with visible reflectance for use in remote sensing of aerosol, IEEE T. Geosci. Remote, 35, 1286–1298, 1997b.

Kaufman, Y. J., Tanré, D., and Boucher, O.: A satellite view of aerosols in the climate system, Nature, 419, 215–223, 2002.

Kittaka, C., Winker, D. M., Vaughan, M. A., Omar, A., and Remer, L. A.: Intercomparison of column aerosol optical depths from CALIPSO and MODIS-Aqua, Atmos. Meas. Tech., 4, 131–141, doi:10.5194/amt-4-131-2011, 2011.

Levy, R. C., Remer, L. A., and Dubovik, O.: Global aerosol optical properties and application to Moderate Resolution Imaging Spectroradiometer aerosol retrieval over land, J. Geophys. Res.-Atmos., 112, D13210, doi:10.1029/2006JD007815, 2007a.

Levy, R. C., Remer, L. A., Mattoo, S., Vermote, E. F., and Kaufman, Y. J.: Second-generation operational algorithm: Retrieval of aerosol properties over land from inversion of Moderate Resolution Imaging Spectroradiometer spectral reflectance, J. Geophys. Res.-Atmos., 112, D13211, doi:10.1029/2006JD007811, 2007b.

Levy, R. C., Remer, L. A., Kleidman, R. G., Mattoo, S., Ichoku, C., Kahn, R., and Eck, T. F.: Global evaluation of the Collection 5 MODIS dark-target aerosol products over land, Atmos. Chem. Phys., 10, 10399–10420, doi:10.5194/acp-10-10399-2010, 2010.

Levy, R. C., Mattoo, S., Munchak, L. A., Remer, L. A., Sayer, A. M., and Hsu, N. C.: The Collection 6 MODIS aerosol products over land and ocean, Atmos. Meas. Tech. Discuss., 6, 159–259, doi:10.5194/amtd-6-159-2013, 2013.

Li, C. C., Lau, A. K. H., Mao, J. T., and Chu, D. A.: Retrieval, validation, and application of the 1-km aerosol optical depth from MODIS measurements over Hong Kong, IEEE T. Geosci. Remote, 43, 2650–2658, 2005.

Li, R.-R., Kaufman, Y. J., Gao, B.-C., and Davis, C. O.: Remote sensing of suspended sediments and shallow coastal waters, IEEE T. Geosci. Remote, 41, 559–566, 2003.

Li, R., Remer, L., Kaufman, Y., Mattoo, S., Gao, B., and Vermote, E.: Snow and ice mask for the MODIS aerosol products, IEEE Geosci. Remote Sens. Lett., 2, 306–310, 2005.

Li, Y., Xue, Y., He, X., and Guang, J.: High resolution aerosol remote sensing retrieval over urban areas by synergetic use of HJ-1 CCD and MODIS data, Atmos. Environ., 46, 173–180, 2012.

Loveland, T. R. and Belward, A. S.: The IGBP-DIS global 1km land cover data set, DISCover: first results, Int. J. Remote Sens., 18, 3289–3295, 1997.

Lyapustin, A., Wang, Y., Laszlo, I., Kahn, R., Korkin, S., Remer, L., Levy, R., and Reid, J. S.: Multiangle implementation of atmospheric correction (MAIAC): 2. Aerosol algorithm, J. Geophys. Res.-Atmos., 116, D03211, doi:10.1029/2010JD014986, 2011.

Martins, J. V., Tanré, D., Remer, L. A., Kaufman, Y. J., Mattoo, S., and Levy, R.: MODIS Cloud Screening for Remote Sensing of Aerosol over Oceans using Spatial Variability, Geophys. Res. Lett., 29, MOD4.1–MOD4.4, doi:10.1029/2001GL013252, 2002.

Oo, M. M., Jerg, M., Hernandez, E., Picon, A., Gross, B. M., Moshary, F., and Ahmed, S. A.: Improved MODIS aerosol retrieval using modified VIS/SWIR surface albedo ratio over urban scenes, IEEE T. Geosci. Remote, 48, 983–1000, 2010.

Quaas, J., Boucher, O., Bellouin, N., and Kinne, S.: Satellite-based estimate of the direct and indirect aerosol climate forcing, J. Geophys. Res., 113, D05204, doi:10.1029/2007JD008962, 2008.

Remer, L. A., Kaufman, Y. J., Tanre, D., Mattoo, S., Chu, D. A., Martins, J. V., Li, R. R., Ichoku, C., Levy, R. C., Kleidman, R. G., Eck, T. F., Vermote, E., and Holben, B. N.: The MODIS aerosol algorithm, products, and validation, J. Atmos. Sci., 62, 947–973, 2005.

Remer, L. A., Kleidman, R. G., Levy, R. C., Kaufman, Y. J., Tanre, D., Mattoo, S., Martins, J. V., Ichoku, C., Koren, I., Yu, H., and Holben, B. N.: Global aerosol climatology from the MODIS satellite sensors, J. Geophys. Res. Atmos., 113, D14S07, doi:10.1029/2007JD009661, 2008.

Remer, L. A., Mattoo, S., Levy, R. C., and Munchak, L.: MODIS 3 km aerosol product: algorithm and global perspective, Atmos. Meas. Tech. Discuss., 6, 69–112, doi:10.5194/amtd-6-69-2013, 2013.

Schmid, B., Michalsky, J., Halthore, R., Beauharnois, M., Harrison, L., Livingston, J., Russell, P., Holben, B., Eck, T., and Smirnov, A.: Comparison of aerosol optical depth from four solar radiometers during the fall 1997 ARM intensive observation period, Geophys. Res. Lett., 26, 2725–2728, 1999.

Smirnov, A., Holben, B. N., Eck, T. F., Dubovik, O., and Slutsker, I.: Cloud screening and quality control algorithms for the AERONET database, Remote Sens. Environ, 73, 337–349, 2000.

Tanré, D., Kaufman, Y. J., Herman, M., and Mattoo, S.: Remote sensing of aerosol properties over oceans using the MODIS/EOS spectral radiances, J. Geophys. Res.-Atmos., 102, 16971–16988, 1997.

van Donkelaar, A., Martin, R. V., and Park, R. J.: Estimating ground-level PM2.5 with aerosol optical depth determined from satellite remote sensing, J. Geophys. Res., 111, D21201, doi:10.1029/2005JD006996, 2006.

Wang, J. and Christopher, S. A.: Intercomparison between satellite-derived aerosol optical thickness and PM2.5 mass: Implications for air quality studies, Geophys. Res. Lett., 30, 2095, doi:10.1029/2003GL018174, 2003.

Atmos. Meas. Tech. Discuss., 6, 1683–1716, 2013
www.atmos-meas-tech-discuss.net/6/1683/2013/
doi:10.5194/amtd-6-1683-2013

Atmospheric Measurement Techniques Discussions

MODIS 3 km aerosol product: applications over land in an urban/suburban region

L. A. Munchak[1,2], R. C. Levy[1,2], S. Mattoo[1,2], L. A. Remer[3], B. N. Holben[1], J. S. Schafer[1,4], C. A. Hostetler[5], and R. A. Ferrare[5]

[1]Earth Science Division, NASA Goddard Space Flight Center, Greenbelt MD 20771, USA
[2]Science Systems and Applications, Inc., Lanham MD 20709, USA
[3]Joint Center for Earth Systems Technology, University of Maryland Baltimore County, Baltimore MD 21228, USA
[4]Sigma Space Corporation, Lanham MD 20706, USA
[5]NASA Langley Research Center, Hampton VA 23681, USA

Received: 31 January 2013 – Accepted: 1 February 2013 – Published: 14 February 2013

Correspondence to: L. A. Munchak (leigh.a.munchak@nasa.gov)

Published by Copernicus Publications on behalf of the European Geosciences Union.

Abstract

MODerate resolution Imaging Spectroradiometer (MODIS) instruments aboard the Terra and Aqua satellites have provided a rich dataset of aerosol information at a 10 km spatial scale. Although originally intended for climate applications, the air quality community quickly became interested in using the MODIS aerosol data. However, 10 km resolution is not sufficient to resolve local scale aerosol features. With this in mind, MODIS Collection 6 is including a global aerosol product with a 3 km resolution. Here, we evaluate the 3 km product over the Baltimore/Washington D.C., USA, corridor during the summer of 2011, by comparing with spatially dense data collected as part of the DISCOVER-AQ campaign; these data were measured by the NASA Langley Research Center airborne High Spectral Resolution Lidar (HSRL) and a network of 44 sun photometers (SP) spaced approximately 10 km apart. The HSRL instrument shows that AOD can vary by up to 0.2 within a single 10 km MODIS pixel, meaning that higher resolution satellite retrievals may help to characterize aerosol spatial distributions in this region. Different techniques for validating a high-resolution aerosol product against SP measurements are considered. Although the 10 km product is more statistically reliable than the 3 km product, the 3 km product still performs acceptably, with more than two-thirds of MODIS/SP collocations falling within the expected error envelope with high correlation ($R > 0.90$). The 3 km product can better resolve aerosol gradients and retrieve closer to clouds and shorelines than the 10 km product, but tends to show more significant noise especially in urban areas. This urban degradation is quantified using ancillary land cover data. Overall, we show that the MODIS 3 km product adds new information to the existing set of satellite derived aerosol products and validates well over the region, but due to noise and problems in urban areas, should be treated with some degree of caution.

AMTD
6, 1683–1716, 2013

1 Introduction

For over twelve years, the MODerate resolution Imaging Spectroradiometer (MODIS) instruments, flying aboard the Terra and Aqua satellites, have been collecting data on the global distribution of climate related variables. Several of these variables describe aerosols, which have been shown to be one of the largest sources of uncertainty in the climate system (IPCC, 2007). MODIS provides a suite of information about aerosol properties, including aerosol optical depth (AOD) and aerosol sizing parameters, that have been used extensively for climate studies (e.g. Kaufman et al., 2002; Bellouin et al., 2005; Quaas et al., 2008). Currently, three algorithms are used operationally to provide products to the public – the dark target algorithm over land (Kaufman et al., 1997a; Levy et al., 2007b, 2010), the dark target algorithm over ocean (Tanré et al., 1997; Remer et al., 2005, 2008) and the deep blue algorithm over land (Hsu et al., 2004, 2006). All produce data at a 10 km nominal spatial scale, which is an appropriate scale for climate studies (Remer et al., 2013).

Soon after launch, it was realized that the retrieved aerosol parameters could be used as proxies for estimating surface air quality conditions (e.g Hutchison, 2003; Wang and Christopher, 2003; Chu et al., 2003; Engels-Cox et al., 2004; Hutchison et al., 2005). The MODIS instruments are particularly appealing for air quality applications because the broad (2330 km) swath of the instrument allows most global locations to be monitored on a nearly daily basis. However, the 10 km resolution of the MODIS aerosol products is insufficient to resolve small-scale features relevant to local air quality, including point sources in urban areas (C. C. Li et al., 2005) and small fire plumes (Lyapustin et al., 2011). Although several research techniques exist to retrieve aerosols at higher spatial scales (100 m to 1 km) from MODIS observations (e.g., Li et al., 2012; Lyapustin et al., 2011), they have not been produced globally in an operational environment.

In response to requests from the air quality community, MODIS Collection 6 will include a global aerosol product at nominal 3 km scale, in addition to the standard

AMTD
6, 1683–1716, 2013

10 km resolution. This 3 km product will include retrievals based on both dark target algorithms (land and ocean). Remer et al. (2013), describe the 3 km product in detail, and analyzed a six-month test database to compare the performance of the 3 km and 10 km products on a global scale. The 3 km product can show more spatial detail than the 10 km product, but agrees less well with ground based sun photometers on a global scale. Accordingly, the 10 km product is still the best choice for studies concerning aerosol effects on climate. However, the 3 km product may be better at characterizing aerosol distributions on local scales, and can only be tested by comparing to dense observations on a small spatial scale. We wish to examine the 3 km aerosol product on a regional scale to determine the additional information content that the higher resolution retrieval provides, and the possible degradation in data quality introduced by moving to a higher resolution.

In this work, we focus primarily on AOD, because it has been used for surface air quality applications (van Donkelaar et al., 2006), and can easily be compared with sunphotometer data. Specifically, we can evaluate AOD products at both 10 km and 3 km resolutions by comparing with surface and airborne-based AOD measurements collected during the DISCOVER-AQ field campaign conducted during the summer of 2011 over the Baltimore-Washington D.C. corridor of the United States. We first assess the similarities and differences in 10 km and 3 km MODIS AOD images, and evaluate whether the 3 km product provides information that is not captured by the 10 km product. We look critically at the best method to validate the higher resolution aerosol retrieval against sun photometer measurements, and validate the 10 km and 3 km products for the campaign duration. The ability of the MODIS product at both 10 km and 3 km resolutions to capture spatial variability in AOD is also addressed. Due to the limited validation data for the over ocean variables, we will only address the land variables in this study.

AMTD
6, 1683–1716, 2013

2 The MODIS 3 km land algorithm

The retrieval method of the global MODIS 3 km aerosol product is thoroughly detailed in Remer et al. (2013). For the sake of completeness, we will briefly describe the land algorithm here. The 3 km algorithm emerges from the "dark target" retrieval methodology (Kaufman et al., 1997a; Tanré et al., 1997; Remer et al., 2005; Levy et al., 2007b, 2013), based on the concept that in the visible wavelengths, aerosols are bright and vegetated surfaces tend to be dark. The spectral contrast between aerosols and the surface can be used to retrieve quantitative information about aerosol properties.

To increase signal-to-noise, the MODIS algorithm retrieves aerosol parameters at a lower spatial resolution than the nominal (at nadir) 500 m top of atmosphere (TOA) reflectance measurements. The algorithm creates N by N "retrieval boxes" of pixels, in order to filter out the subset that is not desirable for aerosol retrieval. Thus, the 10 km algorithm works with 20 × 20 pixel retrieval boxes (400 pixels), whereas the 3 km algorithm works with 6×6 pixel retrieval boxes (36 pixels). Remer et al. (2013) describes how pixels are masked for cloud (Martins et al., 2002), sediments in water (Li et al., 2003), snow and ice (R. Li et al., 2005) and surfaces that are too bright for retrieval. The remaining pixels are sorted by their 0.66 µm reflectance, and the brightest 50 % and darkest 20 % of the remaining pixels are discarded. This means that in the 10 km (3 km) algorithm, there are at most 120 pixels (11 pixels) remaining from which to do aerosol retrieval. The reflectances of these remaining pixels are averaged, resulting in on set of spectral reflectance values to drive the aerosol retrieval. These spectral reflectance values are further "corrected" for gas absorption (e.g. Levy et al., 2013).

The expected "quality" of the retrieval is determined by the number of pixels that remain after all masking and filtering. If at least 51 pixels remain (out of 120) for 10 km or 5 pixels remain (out of 11) for 3 km, then the retrieval is initially expected to be "high" quality. The 10 km retrieval will be attempted if only 12 pixels remain (out of 120), but it is expected to be low quality. There is no corresponding low quality attempt for the 3 km retrieval (Remer et al., 2013).

AMTD
6, 1683–1716, 2013

The over land algorithm performs the retrieval by matching the observed TOA spectral reflectance with lookup tables of pre-computed TOA spectral reflectance. The largest uncertainty is in characterizing the contribution of the surface to the TOA reflectance, for which errors of 0.01 can lead to errors of 0.1 in retrieved AOD. However, Kaufman et al. (1997b) showed that the surface contribution in the 0.47 and 0.66 µm bands can be related to surface contribution in the 2.1 µm shortwave-IR (SWIR) band. The assumed relationship between the visible and SWIR was refined by Levy et al. (2007b), and is used as a constraint in the aerosol retrieval. As described by Levy et al. (2007b), the current retrieval uses the three channels (0.47 µm, 0.66 µm, and 2.1 µm) to determine both the amount of aerosol (total AOD) and the relative ratio of fine and coarse aerosol models. The selection of the fine and coarse aerosol models are prescribed by season and location. The resulting primary retrieved aerosol parameters over land are total AOD at 0.55 µm, the fractional contribution of the fine-dominated aerosol type, the constrained surface reflectance, and fitting error (Levy et al., 2013). All of these assumptions (aerosol lookup tables, assumed surface reflectance relationship, and methodology of the inversion) are identical for both 10 km and 3 km retrievals (e.g. Levy et al., 2013; Remer et al., 2013).

Previously, the MODIS 10 km product has been thoroughly evaluated against sun photometers on global scales. The global expected error (EE) of the 10 km AOD at 0.55 µm product over land is 0.05 ± 0.15 AOD (Remer et al., 2005), and a testbed of 10 km data produced with the Collection 6 MODIS algorithm shows that, globally, 70.6 % of MODIS-Aqua land AOD retrievals fall within this range when collocated and compared to ground based sun photometer measurements (Levy et al., 2013). Remer et al. (2013) has compared the global 3 km MODIS product with sunphotometers and shown that it tends to validate less well than the 10 km. Specifically, since only 62 % of global collocations fell within expected error over land, a new expected error of 0.05 ± 0.25 AOD has been established for the 3 km land product (Remer et al., 2012). Although a new 3 km EE has been established, we choose to continue to use the more

AMTD
6, 1683–1716, 2013

stringent 10 km EE in this paper. Therefore, in this paper, when "EE" is referred to, the 0.05 ± 0.15 AOD definition is employed.

3 Data sources

3.1 MODIS products

This analysis uses five minute sections of the MODIS orbits, termed "granules", collected between 20 June 2011 to 31 July 2011 from both the Aqua and Terra satellites. The level 1B calibrated reflectances for Terra used in the aerosol retrieval were not finalized for collection 6, and may be slightly different from the operational collection 6 level 1B. However, the new calibration technique employed in MODIS Collection 6 is followed in the creation of these level 1B granules.

Additionally, the MODIS land surface cover product (MCD12Q1) is used to characterize surface type. The land cover product uses a trained algorithm to characterize land surface at a 500 m resolution using 5 different classification schemes (Freidl et al., 2010). In this work, we only consider the 17-class International Geosphere-Biosphere Programme (IGBP) system (Loveland and Belward, 1997). Data from both the Terra and Aqua satellites is included in both the training dataset and the product.

3.2 AERONET/DRAGON

The AErosol RObotic NETwork (AERONET) (Holben et al., 1998) has 5 permanent stations operating in the study region. These stations were supplemented with an additional 39 temporary stations, distributed in a roughly 10 km by 10 km grid, termed the Distributed Regional Aerosol Gridded Observation Networks (DRAGON). This network provided an unprecedented opportunity to validate satellite derived aerosol properties at a high spatial resolution. Each station is equipped with a Cimel sun photometer (SP) measuring at eight spectral bands between 340 nm and 1020 nm. AOD is calculated at

AMTD
6, 1683–1716, 2013

550 nm using a quadratic log-log fit (Eck et al., 1999). The AOD retrieval is expected to be accurate to within ±0.015 (Eck et al., 1999; Schmid et al., 1999)

In this work, we use the level 1.5 AERONET/DRAGON SP data, which are cloud screened (Smirnov et al., 2000) but not quality controlled. However, comparisons between level 1.5 and level 2.0 AOD have a correlation of 0.99, a slope of 1 and no offset, and the level 1.5 data contains more measurements.

3.3 High Spectral Resolution LIDAR (HSRL)

The NASA Langley Research Center airborne HSRL instrument calculates aerosol optical depth at 532 nm using independent measurements of vertically resolved aerosol backscatter and extinction, and is therefore expected to be more accurate than a standard backscatter lidar, which typically requires additional data and/or assumptions to produce extinction profiles, and therefore AOD, from the backscatter (Hair et al., 2008). 25 flights were conducted on 13 days between 1 July 2011 and 29 July 2011 on the NASA Langley King Air B200 airplane.

4 Results

4.1 Case studies

Because much of the value of the 3 km resolution retrieval is in better resolving smaller scale aerosol features, we first look at two case studies from differing days in the DISCOVER-AQ study. Figure 1 shows the 10 km (panels a and c) and 3 km (panels b and d) resolution MODIS AOD at 0.55 µm observed by MODIS-Aqua on 21 July 2011 at 18:30 UTC. On this day, there is a strong AOD gradient, with a change from 0.15 to 0.45 AOD over ∼ 50 km, and a local AOD enhancement reaching to over 0.75. HYSPLIT back trajectories, using winds from the NAM model at 12 km resolution, shows that the lower AOD air mass originated in the Midwest, while the higher AOD air mass

AMTD
6, 1683–1716, 2013

was coming from southern Virginia and North Carolina, which had active biomass burning nearby, and also passed over more urbanized regions. The two MODIS products both resolve the AOD gradient, and, in general, show the same aerosol situation. Both products resolve the SP measured AOD maximum of 0.75, although the 3 km product shows more high AOD pixels which may or may not be noise. The 3 km product is able to retrieve closer to clouds, and therefore shows more detail and retrieves more area than the 10 km product. The 3 km product is also able to retrieve over water bodies which are too narrow for 10 km retrievals, and has more pixels near the coastline that are unable to be retrieved by the 10 km product. The ability to retrieve closer to coastline is particularly valuable for air quality applications because many major cities, including some of the largest and most polluted, are located on coasts. This granule not only highlights the value of a high resolution satellite product, but also shows that AOD can vary significantly over small distances.

Plotted overtop of the MODIS AOD images in the circles are MODIS/SP collocations. In all of the panels (a–d), the inner circle shows the SP temporal mean, which is calculated by averaging all SP 0.55 µm measurements at a station within 30 min of the MODIS overpass time, with a minimum of 2 observations. In the top row (panels a and b), the outer circle shows the AOD of the MODIS pixel in which the SP station is located. In the bottom row (panels c and d), the outer circle shows the MODIS spatial mean, which is calculated by averaging all high quality (QA = 3) land pixels within a 5 pixel by 5 pixel box surrounding the SP station requiring at least 5 out of a possible 25 pixels (Ichoku et al., 2002). Therefore, the spatial averaging box for the 3 km product is 15 km by 15 km, and the spatial averaging box for the 10 km product is 50 km by 50 km. The single pixel MODIS collocations in the top row show excellent agreement between the MODIS retrieval and the SP measurements for both the 10 and 3 km products. However, the MODIS spatial average shown in the bottom row gives the impression that the 10 and 3 km products provide different answers; in this case, the smaller averaging box data creates better MODIS/SP agreement for the 3 km product, while the larger averaging box of the 10 km product smoothes out the gradient and causes disagreement.

AMTD
6, 1683–1716, 2013

The spatial averaging does increase the number of MODIS-SP collocations as compared to the single pixel technique, adding 3 collocations for the 3 km product and 2 for the 10 km product. This granule shows that the single pixel collocation technique better characterizes AOD at the SP site, but limits the number of collocations and therefore the statistical robustness of the validation.

Figure 2 shows the 10 km and 3 km resolution MODIS AOD observed by MODIS-Terra on 1 July 2011 at 15:35 UTC, which has a markedly different aerosol distribution than that shown in Fig. 1. On this day, AOD is low (0.11 as measured by the SPs) and is homogeneous across the region. As in Fig. 1, the large-scale view of the two MODIS products agree, but there are nuanced differences. Some noisy pixels are present in the 3 km product, and are less apparent in the 10 km product. Both the 10 km and 3 km products have elevated AOD along the New Jersey and Delaware coastline, which are plausibly cloud contaminated from sub pixel clouds. The 10 km has fewer contaminated pixels, but they extend further from the coastline; the 3 km product has more contaminated pixels, but their spatial extent is limited to right along the coastline. The 3 km product also shows some striping that results from differences in the MODIS instrument detectors. As in Fig. 1, the 3 km product has more coverage over the water areas in this scene. The MODIS/SP collocation circles are as they were in Fig. 1, with MODIS single pixel collocations shown in the outer circles of the top row, MODIS spatial average collocations in the outer circles of the bottom row, and SP temporal averages in the inner circle of all panels.

In this aerosol situation, the spatial averaging of the 10 km product AOD increases the agreement with the SP measurements because the averaging decreases the impact of noisy pixels. 30 out of the 31 collocations shown in Fig. 2c fall within expected error, and the average retrieved 0.55 µm AOD at the SP stations is 0.10, only 0.01 lower than the SP determined AOD. The MODIS 3 km spatially averaged collocations show an AOD enhancement of 0.1 to 0.3 over Baltimore City that is not observed by the SP measurements; 6 out of the 28 MODIS 3 km spatial averages are above expected error. The largest difference between the MODIS 3 km retrieved AOD & SP measured

AMTD
6, 1683–1716, 2013

AOD was observed at the AERONET/DRAGON station in Essex, Maryland, 13 km east of downtown Baltimore, where the SP AOD is 0.11, and the AOD of the 3 km spatial average is 0.41. A similar AOD enhancement is seen over the Washington D.C., although there are no SP measurements to confirm that this enhancement is a retrieval artifact. The single MODIS pixel collocations in the Fig. 2b do not capture this important retrieval problem due to the coincidences of where the AERONET stations happen to be located and if the exact pixel where the station is located is retrieved. This case study suggests that the spatial average collocation technique better characterizes the retrieval performance over the larger region, and the single pixel collocation technique may misrepresent product performance because it is much more sensitive to the siting of the SP stations.

The airborne HSRL measurements provide an opportunity to look at aerosol extinction and AOD spatial variability with an nominal 1 min resolution, which corresponds to a nearly 6 km horizontal resolution. Figure 3 shows another high aerosol loading day, observed by MODIS-Terra on 29 July 2011 at 16:00 UTC. HSRL 532 nm columnar AOD along the flight track between 15:30 and 16:30 UTC is shown in the thick line, plotted atop of the 3 km resolution 0.55 µm AOD. The sections of the flight track where the plane was flying lower than 7 km, flying above clouds, or was turning are shown in grey. SP AOD interpolated to 0.55 µm is shown in the circles. The AERONET measurements are not temporally averaged; the nearest measurement to 16:00 UTC is used, provided the measurement was taken between 15:30 and 16:30 UTC.

The SP AOD measurements range from 0.33 to 0.58, with lower values towards the south and west, and higher values towards the north and east. The HSRL AOD measurements have a wider range from 0.35 to 0.67. There is excellent agreement between HSRL and SP measurements at the AERONET stations, which indicates that the broader range of AOD values from HSRL than from AERONET is likely due to the HSRL instrument being able to measure a larger area and not due to inaccuracies in either measurement. The MODIS 3 km product generally captures the spatial pattern of AOD as observed by both the HSRL instrument and the AERONET stations, although

AMTD
6, 1683–1716, 2013

as in Fig. 2, the AOD is overestimated in the urban areas and there are noisy retrievals. Outside of the urban areas, the MODIS image shows AOD near 0.4 for much of the southern and western portion of the granule, increasing for 0.65 in the northeastern portion of the granule that also has HSRL and SP measurements. Overall, the three instruments show a rather similar aerosol situation albeit with varying levels of detail.

The HSRL AOD measurements reflect the more general pattern observed by AERONET, but also show many small-scale enhancements that cannot be observed even with the high spatial density of the DRAGON network. The western portion of the flight track in Fig. 4 shows that the HSRL instrument measured an increase in AOD from 0.41 to 0.59 over ∼ 4 min between 16:00:08 and 16:04:28 UTC, and traveling south by 29.8 km and west by 5.3 km in this time period . This change takes place over three 10 km boxes and ten 3 km boxes. The MODIS 3 km product successfully replicates the absolute change in AOD, although the gradient along the flight track is not exactly reproduced because of missing and noisy pixels. The maximum AOD is overestimated in the 10 km product, and is retrieved exactly in the 3 km product, although a neighboring pixel has an anomalously high AOD. It is probable that there is a source of contamination in the noisy 3 km pixel, which was included in the 10 km pixel along with the good pixels, resulting in an overestimation in the 10 km pixel. From this comparison, it is clear that while the 3 km product contains more noisy pixels that are likely contaminated, the smaller pixel size limits the spatial extent of the contamination and allows nearby uncontaminated pixels to retrieve the correct AOD. In the 3 km product, the effects of cloud or surface contamination are larger within a single pixel, but at the same time are also spatially limited.

As highlighted in Fig. 4, because the HSRL instrument makes several measurements within a single MODIS pixel, it provides an opportunity to assess AOD variability across the standard MODIS retrieval resolution. A measure of subpixel AOD variability is shown in Fig. 5. For each 10 km resolution MODIS pixel, the minimum HSRL measured AOD is subtracted from the maximum HSRL AOD, provided the measurements are within half an hour of the MODIS overpass. Data from all flights that have valid data

AMTD
6, 1683–1716, 2013

within half an hour of a MODIS overpass are included, and only MODIS pixels that contain more than 5 HSRL observations are analyzed to ensure that two fully independent HSRL measurements are obtained within the MODIS pixel. 410 MODIS pixels are able to be analyzed for subpixel AOD variations. Within a single MODIS 10 km pixel, the maximum HSRL measured AOD change is 0.25, increasing from 0.36 to 0.61 AOD. The mean 0.55 µm AOD variation within a 10 km pixel is 0.037 while the median variation within a 10 km pixel is 0.023. Fewer than 25 % of pixels contained less than 0.01 AOD variation. The 10 km retrieval assumes uniformity of the AOD across the retrieval box, and that is simply not the case. The assumption is likely to hold better across the 3 km retrieval box; however, the nominal resolution of the HSRL instrument for this study is larger than the 3 km retrieval box. For this case, decreasing the HSRL nominal horizontal resolution for AOD from 6 km to 1 km increased the noise to an unacceptably high level such that the AOD variation within the MODIS 3 km pixels could not be quantified.

The case study comparisons with ground and airborne based AOD measurements show that the MODIS 3 km product contains additional aerosol information as compared to the 10 km product. Figure 1 shows a situation in which a few high AOD pixels in the 10 km product could be interpreted as noise, but the higher resolution of the 3 km product provides many more pixels, and SP data confirms that a true high aerosol loading event was identified. Additionally, the 3 km retrieval is able to retrieve over small water bodies and close to coastline. The sub-pixel AOD variability observed by HSRL suggests that a 10 km product will frequently miss small changes in AOD over an urban/suburbam region. However, retrieving with a higher resolution reduces the statistical robustness of the aerosol product, resulting in more noise and inaccurate retrievals over urban areas.

4.2 MODIS 3 km validation

The case studies highlight the strengths and weaknesses of the 3 km product; however, the sun photometer data from the entire campaign provides the most comprehensive dataset to characterize the performance of the 3 km product. The SP data also allows

AMTD
6, 1683–1716, 2013

a critical look at how the different collocation techniques demonstrated in Figs. 1 and 2 lead to different conclusions on the validity on the MODIS AOD data in this region for both the 10 and 3 km resolutions.

In Fig. 6a, all 3 km MODIS/SP 0.55 µm AOD collocations are shown in a density scatterplot, using the MODIS single pixel collocation technique employed in Figs. 1b and 2b. In Fig. 6b, these single pixel MODIS/SP collocations are binned by the SP AOD, and the mean MODIS-SP difference for the bin is plotted for both the 10 and 3 km products. This process is repeated in Fig. 6c and d except that the 5×5 pixel MODIS spatial collocation technique is employed in the MODIS/SP collocations.

For both MODIS/SP collocation techniques, the bulk of the 3 km MODIS retrievals are within the $\pm 0.05 \pm 0.15$ AOD expected error (67 % for the single pixel technique and 73 % for the spatial average technique). The satellite retrieval is highly correlated with the ground based measurements, although with a small negative offset (−0.02 for the single pixel technique and −0.01 for the spatial average technique) and a significant slope (1.26 for single pixel, 1.22 for spatial average). Accordingly, the MODIS 3 km AOD agrees well with SP AOD at low aerosol loadings, but is generally biased high at higher AOD. The primary difference between the two collocation techniques is that the spatial average has nearly twice as many collocations (962 as opposed to 560). Therefore, the spatial averaging technique may be more representative of the region at large.

The binned MODIS-SP differences in Fig. 6b and d agree well with the impression given by the scatterplots. The MODIS 3 km product is biased slightly low at AOD below 0.1, then is biased high above 0.1. The single pixel collocation is likely best to compare the 10 km and 3 km products, because the spatial averaging technique samples a different area for the different products. The 3 km product single pixel averages shown in Fig. 6b show that the average AOD of the 3 km product is frequently, but not always, higher than the 10 km product for bins above 0.1 AOD.

The retrieved AOD from the HSRL airborne instrument provides a different perspective on validation of the 3 km product. Because the plane is moving quickly in space, no spatial or temporal averaging is used to make the MODIS/HSRL collocations. The

AMTD
6, 1683–1716, 2013

MODIS data are sampled along the HSRL flight track, provided that the HSRL observation is made within the geographic region mapped in Figs. 1 and 2, and is within 30 min of the MODIS overpass. Shortening the time requirement to either 15 or 5 min does not significantly affect the collocation statistics, but provides far fewer collocations. The HSRL and MODIS AOD are not interpolated to the same wavelength, which is expected to introduce between 2–4 % error (Kittaka et al., 2011). It is expected that the AOD retrieved by the HSRL instrument would be lower than the AOD retrieved by MODIS by at least 0.01 to 0.02 because the HSRL instrument does not measure the entire column, and therefore neglects the contribution of above the HSRL profile (i.e. above 7 km) to total columnar AOD.

Figure 7 shows that the 3 km product agrees well with HSRL, although less well than the 10 km product. Although both MODIS products are biased high in this region during the study period, the 3 km product is moreso; the bias of the 10 km product is 0.050 while the bias of the 3 km product is 0.056. The increased bias of the 3 km is primarily attributed to the addition of noisy pixels that the 10 km product avoids during its pixel selection process. Although the 10 km product has better statistical agreement with HSRL, the 10 km MODIS/HSRL comparison also shows the necessity of a higher resolution retrieval; the stripes in the HSRL/MODIS comparison show the change in HSRL AOD within a single pixel – the pattern that is quantified in Fig. 5.

From both AERONET and HSRL comparisons, we consider the 3 km product to be well validated in this region. Using either collocation technique, more than two thirds of MODIS/SP collocations are within the expected error of the 10 km product, which is more stringent than the defined EE of the 3 km product. However, the increased noise and urban problems give the 3 km product a larger high bias than the 10 km product. The single pixel and spatial average MODIS collocation techniques show quantitative but not qualitative differences.

AMTD
6, 1683–1716, 2013

4.3 Sources of uncertainty

Figures 2 and 3 show an overestimation of AOD in urban areas. In order to study this further, we separate the 3 km MODIS/SP spatially averaged collocations by SP station, and compute agreement statistics for each station. We choose the spatial averaging collocation technique because it provides more collocations. The percent of comparisons within expected error for each station is shown in Fig. 8a, and the correlation coefficient (R) between MODIS and SP 0.55 µm AOD is shown in Fig. 8b. In each panel, land classified as "urban" by the MODIS Land Cover type product (MCD12Q1) is plotted in grey.

Figure 8a shows remarkable variability in the percent of collocations within EE for each SP station, ranging between 16 % to 95 %. The stations with the smallest percent within EE are clustered around the Baltimore urban center, and the more urbanized I-95 corridor between Washington D.C. and Baltimore. However, the stations with small percentages of collocations within EE still have correlation coefficients above 0.85, suggesting that the error is a systematic bias that could be accounted for in future retrievals, and not a random error.

We wish to quantify the urban overestimation of the 3 km product using the dense spatial distribution of the SP sites. Using the same 15 km averaging box as the MODIS spatial collocation, the percent of pixels within the averaging box identified as urban by the MCD12Q1 product is calculated. In Fig. 9, this quantity is plotted against the percent of collocations above EE for each SP site. The percent of urban land within the MODIS averaging box is well correlated with the percent of MODIS/SP collocations that are above the expected error. This confirms that the largest source of uncertainty in this study is related to the urban areas. The cause is suspected to be improper land surface reflectance characterization, considering that aerosol sources are not expected to vary significantly within the region of study and that it has been shown that the surface reflectance in the 0.66 um channel over some urban surfaces is ~ 0.7 of the 2.13 reflectance (Castanho et al., 2008; Oo et al., 2010) which is higher than the ratio

AMTD
6, 1683–1716, 2013

used in the MODIS operational retrievals. In mixed-use urban/suburban regions like the DISCOVER-AQ study region, it is likely that the brighter urban surface 500 m pixels were selectively discarded in the pixel selection process of the 10 km product. However, because the resolution of the 3 km retrieval is smaller, more urban pixels remain within the retrieval box after pixel selection, causing the surface reflectance in the visible wavelengths to be underestimated, leading to an overestimation in AOD.

Ideally, the noisy pixels could be flagged as poor quality, and therefore treated with some degree of caution. One of the products produced operationally is the AOD at 2.1 µm. This is not a validated product, but is used as a diagnostic to the retrieval. It may hold information that can identify poorer quality 3 km retrievals. In Fig. 10a, the 2.1 µm AOD on 21 July 2011 at 18:30 from the 3 km product is plotted, the same granule as shown in Fig. 1b, and in Fig. 10b, the 2.1 µm AOD on 1 July 2011 at 15:35 from the 3 km product is plotted, the same granule as shown in Fig. 2b. The scene-wide 2.1 µm AOD is 0.042 in the left panel, and is 0.03 in the right panel. Both granules contain pixels with a 2.1 µm AOD over 0.2, more than 6 to 10 times higher than the scene-wide average. The error is not due to the wrong aerosol model being picked; in both scenes; all of the pixels were assigned the fine mode dominated urban aerosol model (Levy et al., 2007a). It appears that the same pixels that have anomalously high 2.1 µm AOD retrievals also tend to have inaccurate 0.55 µm AOD retrievals. For example, the pixels with high (>0.55) AOD in Fig. 1b that agree with SP observations have retrieved 2.1 µm AOD values that do not stand out from the background. However, the pixels with high AOD in Fig. 2b that do not agree with SP observations, exhibit retrieved 2.1 µm AOD values significantly higher than the background. Although the 2.1 µm AOD retrieval is an unvalidated product, it may serve a purpose as a consistency check in this fine mode dominated, urban environment. This consistency check is likely to be inapplicable in dusty or other coarse mode dominated regimes.

Using anomalous 2.1 µm AOD pixels as a proxy for poor quality 0.55 µm pixels, and therefore throwing them out, results in a reduction of the both the negative bias at low AOD and the positive bias at high AOD. If the 3 km product is filtered such that

AMTD
6, 1683–1716, 2013

pixels with a 2.1 µm AOD over 0.2 are excluded, and MODIS/SP are collocated using the spatial averaging technique, the percent within EE rises from 73 % to 80 %, while the number of collocations falls from 963 to 903, and the R rises from 0.92 to 0.95. However, this screening is not globally applicable, and is not recommended for use without closer examination.

It appears that a primary source of error in the 3 km MODIS aerosol product is the incorrect estimation of surface reflectance over urban regions. This error is not as apparent in the 10 km product because brighter urban surfaces are preferentially discarded during the pixel selection process. However, because the 3 km product has a smaller footprint, it is likely that not all urban pixels are discarded, and the surface reflectance is underestimated, leading to an overestimation in AOD. The 2.1 µm AOD shows some potential as an imperfect filter for these poor quality pixels.

5 Summary and conclusions

The MODIS dark target aerosol algorithms were designed with climate applications in mind, and the spatial scale of the retrieval reflects that design. However, as the applications of the aerosol product have evolved to include many facets of air quality studies, the proper scale at which to observe small-scale aerosol events came into question. In response to the needs of the air quality community, an operational aerosol product produced at a 3 km resolution will be available in MODIS Collection 6.

This new product was evaluated against ground and airborne data over the Baltimore-Washington D.C., USA corridor over the summer of 2011 to understand the potential added information from the higher resolution retrieval and the statistical reliability of the product. The 10 km and 3 km granules generally resolve similar large scale patterns in aerosol distribution but differ in the details. The smaller footprint of the 3 km product retrieves closer to clouds and over small bodies of water, but also makes the product more susceptible to cloud contamination and other sources of noise. Sub-pixel comparisons against HSRL shows that AOD can vary significantly within a 10 km pixel,

AMTD
6, 1683–1716, 2013

and a 3 km resolution is an appropriate scale for studying aerosol distributions in urban and suburban settings.

The dense network of AERONET sun photometers deployed during the DISCOVER-AQ campaign provided an unprecedented opportunity to validate aerosol products at a high spatial scale. Given the new resolution of both the satellite data and the ground validation network, the MODIS spatial-temporal collocation techniques for validation were revisited. It was found that using a spatial average of MODIS pixels around a sun photometer station, or using only the pixel where the SP station is located resulted in a quantitative, but not qualitative, difference. We conclude with good confidence that the MODIS 3 km validates within the expected error of the MODIS aerosol products in this region, but is biased high at AOD values greater than 0.1.

There is evidence that a significant source of the bias observed in the 3 km product results from improper characterization of urban surfaces. The method for attributing the surface contributions to TOA measured reflectances has been documented to underestimate the surface reflectances in urban areas (Castanho et al., 2008; Oo et al., 2010), which in turn overestimates AOD. Indeed, we found a strong correlation between the amount of urban surface near an AERONET station, and the percent of collocations that are above the expected error. While case studies show that the 10 km product also has one or two pixels that are affected, the smaller pixel size of the 3 km product causes it to be more susceptible to contamination.

The poor performance of the 3 km product over urban surfaces is clearly a limitation in terms of air quality applications. How to best address this problem in an operational environment remains an open question. However, despite this limitation, the 3 km product has many qualities making it a suitable choice for air quality studies, including resolving small scale AOD gradients and point sources, the ability to retrieve in patchy cloud fields, and the ability to retrieve closer to coastlines. We expect that the added information of the 3 km resolution product will complement the existing MODIS 10 km resolution aerosol product and products from other passive and active sensors to provide a more complete view of global aerosol properties from space.

AMTD
6, 1683–1716, 2013

Acknowledgements. The authors thank Bill Ridgeway and the MODAPS team for facilitating iterative testing needs. We also thank the University of Wisconsin PEATE team for the production of the Terra L1B data used in this study. We recognize the entire AERONET team for their efforts to deploy and maintain 44 functioning AERONET stations. HSRL operations were funded by the NASA DISCOVER-AQ program. The authors also thank the NASA Langley King Air King Air flight crew for their outstanding work supporting these flights.

References

Bellouin, N., Boucher, O., Haywood, J., and Reddy, M. S.: Global estimate of aerosol direct radiative forcing from satellite measurements, Nature, 438, 1138–1141, 2005.

Castanho, A. D., Martins, J. V., and Artaxo, P.: MODIS Aerosol Optical Depth Retrievals with high spatial resolution over an Urban Area using the Critical Reflectance, J. Geophys. Res., 113, D02201, doi:10.1029/2007JD008751, 2008.

Chu, D. A.: Global monitoring of air pollution over land from the Earth Observing System-Terra Moderate Resolution Imaging Spectroradiometer (MODIS), J. Geophys. Res., 108, 4661, doi:10.1029/2002JD003179, 2003.

Drury, E., Jacob, D. J., Wang, J., Spurr, R. J., and Chance, K.: Improved algorithm for MODIS satellite retrievals of aerosol optical depths over western North America, J. Geophys. Res., 113, D16204, doi:10.1029/2007JD009573, 2008.

Eck, T. F., Holben, B. N., Reid, J. S, Dubovik, O., Smirnov, A., O'Neill, N. T., Slutsker, I., and Kinne, S.: Wavelength dependence of the optical depth of biomass burning, urban and desert dust aerosols, J. Geophys. Res., 104, 31333–31350, 1999.

Engel-Cox, J. A., Holloman, C. H., Coutant, B. W., and Hoff, R. M.: Qualitative and quantitative evaluation of MODIS satellite sensor data for regional and urban scale air quality, Atmos. Environ., 38, 2495–2509, 2004.

Evans, K. and Stephens, G.: A new polarized atmospheric radiative-transfer model, J. Quant. Spectrosc. Ra., 46, 413–423, 1991.

Friedl, M. A., Sulla-Menashe, D., Tan, B., Schneider, A., Ramankutty, N., Sibley, A., and Huang, X.: MODIS Collection 5 global land cover: Algorithm refinements and characterization of new datasets, Remote Sens. Environ., 114, 168–182, 2010.
Hair, J. W., Hostetler, C. A., Cook, A. L., Harper, D. B., Ferrare, R. A., Mack, T. L., Welch, W., Izquierdo, L. R., and Hovis, F. E.: Airborne high spectral resolution LIDAR for profiling aerosol optical properties, Appl. Optics, 47, 6734–6752, 2008.
Holben, B. N., Eck, T. F., Slutsker, I., Tanré, D., Buis, J. P., Setzer, A., Vermote, E., Reagan, J. A., Kaufman, Y. J., Nakajima, T., Lavenu, F., Janowiak, I., and Smirnov, A.: AERONET – A federated instrument network and data archive for aerosol characterization, Remote Sens. Environ., 66, 1–16, 1998.
Hsu, N. C., Tsay, S. C., King, M. D., and Herman, J. R.: Aerosol Properties Over Bright-Reflecting Source Regions, IEEE T. Geosci. Remote, 42, 557–569, 2004.
Hsu, N. C., Tsay, S. C., King, M. D., and Herman, J. R.: Deep blue retrievals of Asian aerosol properties during ACE-Asia, IEEE T. Geosci. Remote, 44, 3180–3195, 2006.
Hutchison, K. D.: Applications of MODIS satellite data and products for monitoring air quality in the state of Texas, Atmos. Environ., 37, 2403–2412, 2003.
Hutchison, K. D., Smith, S., and Faruqui, S.: The use of MODIS data and aerosol products for air quality prediction, Atmos. Environ., 38, 5057–5070, 2004.
Ichoku, C., Chu, D. A., Mattoo, S., Kaufman, Y. J., Remer, L. A., Tanré, D., Slutsker, I., and Holben, B. N.: A spatio-temporal approach for global validation and analysis of MODIS aerosol products, Geophys. Res. Lett., 29, 1.1–1.4, doi:10.1029/2001GL013206, 2002.
IPCC: AR4 WG1, Climate Change 2007: The Physical Science Basis, Contribution of Working Group I to the Fourth Assessment Report of the Intergovernmental Panel on Climate Change, edited by: Solomon, S., Qin, D., Manning, M., Chen, Z., Marquis, M., Averyt, K. B., Tignor, M., and Miller, H. L., Cambridge University Press, ISBN 978-0-521-88009-1, 2007.
Kaufman, Y. J., Tanré, D., Remer, L., Vermote, E., Chu, A., and Holben, B.: Operational remote sensing of tropospheric aerosol over land from EOS moderate resolution imaging spectroradiometer, J. Geophys. Res., 102, 17051–17067, 1997a.
Kaufman, Y. J., Wald, A., Remer, L., Gao, B., Li, R., and Flynn, L.: The MODIS 2.1 µm channel – Correlation with visible reflectance for use in remote sensing of aerosol, IEEE T. Geosci. Remote, 35, 1286–1298, 1997b.

AMTD
6, 1683–1716, 2013

Kaufman, Y. J., Tanré, D., and Boucher, O.: A satellite view of aerosols in the climate system, Nature, 419, 215–223, 2002.
Levy, R. C., Remer, L. A., and Dubovik, O.: Global aerosol optical properties and application to Moderate Resolution Imaging Spectroradiometer aerosol retrieval over land, J. Geophys. Res.-Atmos., 112, D13210, doi:10.1029/2006JD007815, 2007a.
Levy, R. C., Remer, L. A., Mattoo, S., Vermote, E. F., and Kaufman, Y. J.: Second-generation operational algorithm: Retrieval of aerosol properties over land from inversion of Moderate Resolution Imaging Spectroradiometer spectral reflectance, J. Geophys. Res.-Atmos., 112, D13211, doi:10.1029/2006JD007811, 2007b.
Levy, R. C., Remer, L. A., Tanré, D., Mattoo, S., and Kaufman, Y. J.: Algorithm for remote sensing of dark targets from MODIS: Collections 005 and 051: Revision 2; February 2009, MODIS Algorithm Theoretical Basis Document, 2009.
Levy, R. C., Remer, L. A., Kleidman, R. G., Mattoo, S., Ichoku, C., Kahn, R., and Eck, T. F.: Global evaluation of the Collection 5 MODIS dark-target aerosol products over land, Atmos. Chem. Phys., 10, 10399–10420, doi:10.5194/acp-10-10399-2010, 2010.
Levy, R. C., Mattoo, S., Munchak, L. A., Remer, L. A., Sayer, A. M., and Hsu, N. C.: The Collection 6 MODIS aerosol products over land and ocean, Atmos. Meas. Tech. Discuss., 6, 159–259, doi:10.5194/amtd-6-159-2013, 2013.
Li, C. C., Lau, A. K. H., Mao, J. T., and Chu, D. A.: Retrieval, validation, and application of the 1-km aerosol optical depth from MODIS measurements over Hong Kong, IEEE T. Geosci. Rem., 43, 2650–2658, 2005.
Li, R., Remer, L., Kaufman, Y., Mattoo, S., Gao, B., and Vermote, E.: Snow and ice mask for the MODIS aerosol products, IEEE Geosci. Remote S., 2, 306–310, 2005.
Li, R.-R., Kaufman, Y. J., Gao, B.-C., and Davis, C. O.: Remote sensing of suspended sediments and shallow coastal waters, IEEE T. Geosci. Remote, 41, 559–566, 2003.
Li, Y., Xue, Y., He, X., and Guang, J.: High resolution aerosol remote sensing retrieval over urban areas by synergetic use of HJ-1 CCD and MODIS data, Atmos. Environ., 46, 173–180, 2012.
Loveland, T. R. and Belward, A. S.: The IGBP-DIS global 1km land cover data set, DISCover: first results, Int. J. Remote Sens., 18, 3289–3295, 1997.
Lyapustin, A., Wang, Y., Laszlo, I., Kahn, R., Korkin, S., Remer, L., Levy, R., and Reid, J. S.: Multiangle implementation of atmospheric correction (MAIAC): 2. Aerosol algorithm, J. Geophys. Res.-Atmos., 116, D03211 doi:10.1029/2010JD014986, 2011.

AMTD
6, 1683–1716, 2013

Martins, J. V., Tanré, D., Remer, L. A., Kaufman, Y. J., Mattoo, S., and Levy, R.: MODIS Cloud Screening for Remote Sensing of Aerosol over Oceans using Spatial Variability, Geophys. Res. Lett., 29, 4.1–4.4, doi:10.1029/2001GL013252, 2002.

Oo, M. M., Jerg, M., Hernandez, E., Picon, A., Gross, B. M., Moshary, F., and Ahmed, S. A.: Improved MODIS aerosol retrieval using modified VIS/SWIR surface albedo ratio over urban scenes, IEEE T. Geosci. Remote, 48, 983–1000, 2010.

Quaas, J., Boucher, O., Bellouin, N., and Kinne, S.: Satellite-based estimate of the direct and indirect aerosol climate forcing, J. Geophys. Res., 113, D05204, doi:10.1029/2007JD008962, 2008.

Remer, L. A., Kaufman, Y. J., Tanré, D., Mattoo, S., Chu, D. A., Martins, J. V., Li, R. R., Ichoku, C., Levy, R. C., Kleidman, R. G., Eck, T. F., Vermote, E., and Holben, B. N.: The MODIS aerosol algorithm, products, and validation, J. Atmos. Sci., 62, 947–973, 2005.

Remer, L. A., Kleidman, R. G., Levy, R. C., Kaufman, Y. J., Tanré, D., Mattoo, S., Martins, J. V., Ichoku, C., Koren, I., Yu, H., and Holben, B. N.: Global aerosol climatology from the MODIS satellite sensors, J. Geophys. Res. Atmos., 113, D14S07, doi:10.1029/2007JD009661, 2008.

Remer, L. A., Mattoo, S., Levy, R. C., and Munchak, L.: MODIS 3 km aerosol product: algorithm and global perspective, Atmos. Meas. Tech. Discuss., 6, 69–112, doi:10.5194/amtd-6-69-2013, 2013.

Rogers, R. R., Hair, J. W., Hostetler, C. A., Ferrare, R. A., Obland, M. D., Cook, A. L., Harper, D. B., Burton, S. P., Shinozuka, Y., McNaughton, C. S., Clarke, A. D., Redemann, J., Russell, P. B., Livingston, J. M., and Kleinman, L. I.: NASA LaRC airborne high spectral resolution lidar aerosol measurements during MILAGRO: observations and validation, Atmos. Chem. Phys., 9, 4811–4826, doi:10.5194/acp-9-4811-2009, 2009.

Schmid, B., Michalsky, J., Halthore, R., Beauharnois, M., Harrison, L., Livingston, J., Russell, P., Holben, B., Eck, T., and Smirnov, A.: Comparison of aerosol optical depth from four solar radiometers during the fall 1997 ARM intensive observation period, Geophys. Res. Lett., 26, 2725–2728, 1999.

Tanré, D., Kaufman, Y. J., Herman, M., and Mattoo, S.: Remote sensing of aerosol properties over oceans using the MODIS/EOS spectral radiances, J. Geophys. Res.-Atmos., 102, 16971–16988, 1997.

AMTD
6, 1683–1716, 2013

van Donkelaar, A., Martin, R. V., and Park, R. J.: Estimating ground-level $PM_{2.5}$ with aerosol optical depth determined from satellite remote sensing, J. Geophys. Res., 111, D21201, doi:10.1029/2005JD006996, 2006.

Wang, J. and Christopher, S. A.: Intercomparison between satellite-derived aerosol optical thickness and $PM_{2.5}$ mass: Implications for air quality studies, Geophys. Res. Lett., 30, 2095, doi:10.1029/2003GL018174, 2003.

AMTD

6, 1683–1716, 2013

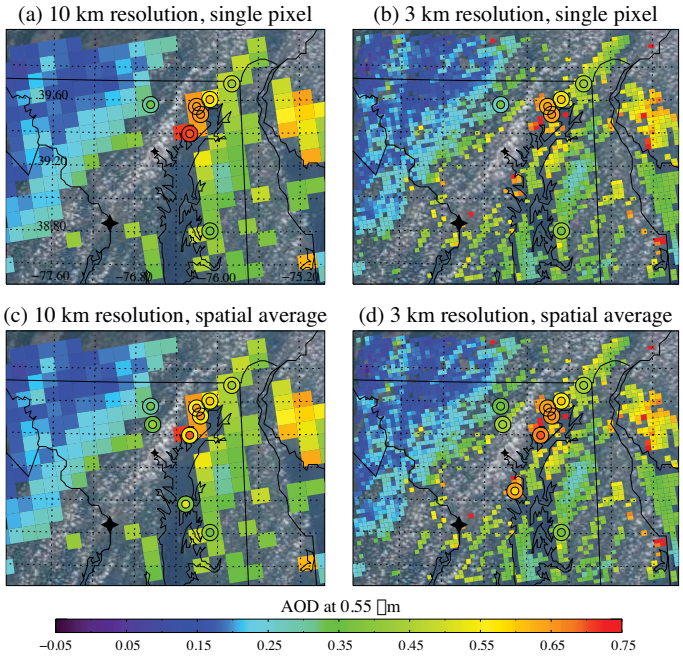

Fig. 1. AOD at 0.55 µm observed by MODIS-Aqua on 21 July 2011 at 18:30 UTC is plotted at the 10 km resolution (**a**, **c**) and 3 km resolution (**b**, **d**). MODIS/SP collocations are plotted in the circles. In **(a)**–**(d)**, the inner circle is the SP temporally averaged AOD, which is average of ≥ 2 SP measurements within 30 min of MODIS overpass. In **(a)** and **(b)**, the outside circle is the AOD of the MODIS pixel containing the SP site. In **(c)** and **(d)**, the outer circle is a the spatial average of a MODIS AOD in a 5 × 5 pixel box around the SP station. Only land pixels with a QA = 3 are used in the collocation. Washington D.C. is shown with the large black star and Baltimore, MD is shown with the small black star. The true color image, created from the MODIS red, green and blue bands, is shown in the background.

AMTD
6, 1683–1716, 2013

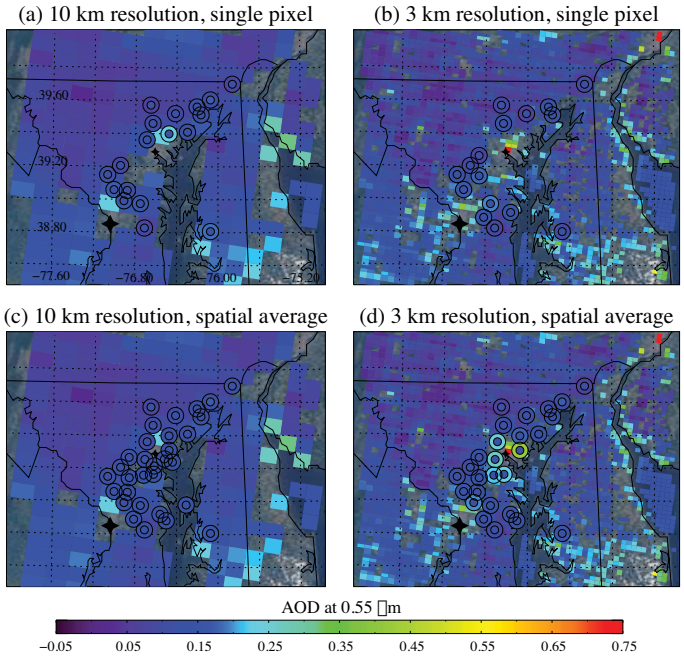

Fig. 2. AOD at 0.55 µm observed by MODIS-Terra on 1 July 2011 at 15:35 UTC is plotted at the 10 km resolution (**a**, **c**) and 3 km resolution (**b**, **d**). MODIS/SP collocations are plotted in the circles. In **(a)**–**(d)**, the inner circle is the SP temporally averaged AOD, which is average of ≥ 2 SP measurements within 30 min of MODIS overpass. In **(a)** and **(b)**, the outside circle is the AOD of the MODIS pixel containing the SP site. In **(c)** and **(d)**, the outer circle is a the spatial average of a MODIS AOD in a 5 × 5 pixel box around the SP station. Only land pixels with a QA = 3 are used in the collocation. Washington D.C. is shown with the large black star and Baltimore, MD is shown with the small black star. The true color image, created from the MODIS red, green and blue bands, is shown in the background.

AMTD
6, 1683–1716, 2013

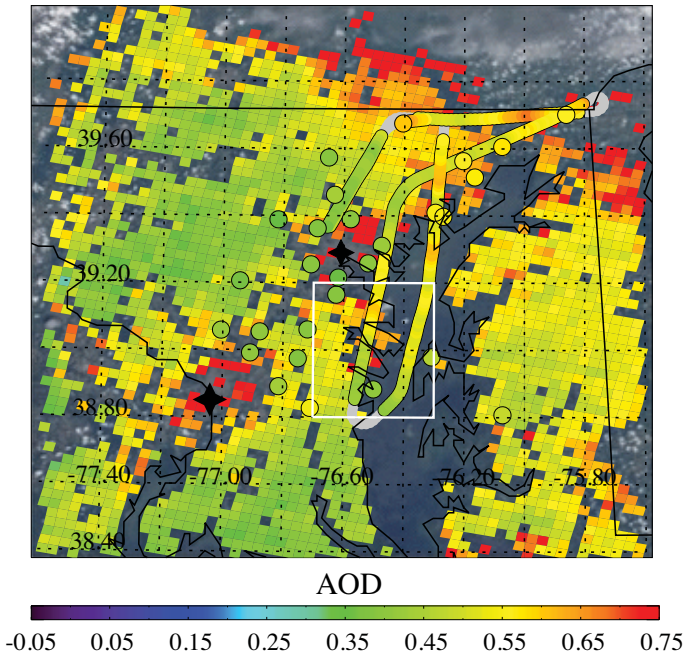

Fig. 3. 3 km resolution AOD at 0.55 µm observed by MODIS-Terra on 29 July 2011 at 16:00 UTC is plotted in the background. HSRL 532 nm columnar AOD along the flight track between 15:30 and 16:30 UTC is shown in the thick line. SP AOD interpolated to 0.55 µm is shown in the circles. The SP measurements are not temporally averaged; the nearest measurement to 16:00 UTC is shown, provided the measurement was taken between 15:30 and 16:30 UTC. Washington D.C. is shown with the large black star and Baltimore, MD is shown with the small black star. The true color image, created from the MODIS red, green and blue bands, is shown in the background.

AMTD
6, 1683–1716, 2013

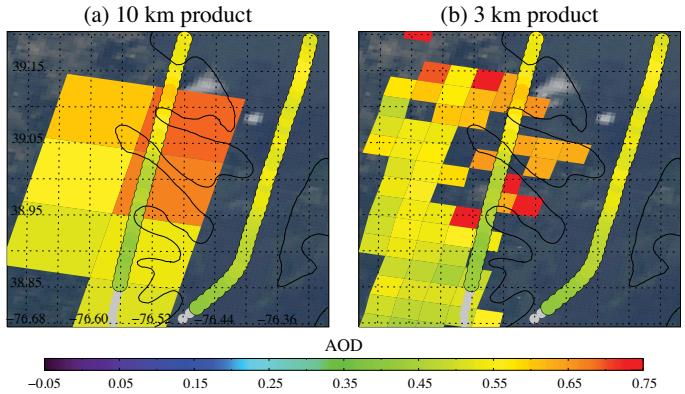

Fig. 4. Close up view of the area enclosed in the white box in Fig. 3. **(a)** MODIS 10 km 0.55 µm AOD with 532 nm HSRL AOD plotted on top. **(b)** MODIS 3 km 0.55 µm AOD with 532 nm HSRL AOD plotted on top.

AMTD
6, 1683–1716, 2013

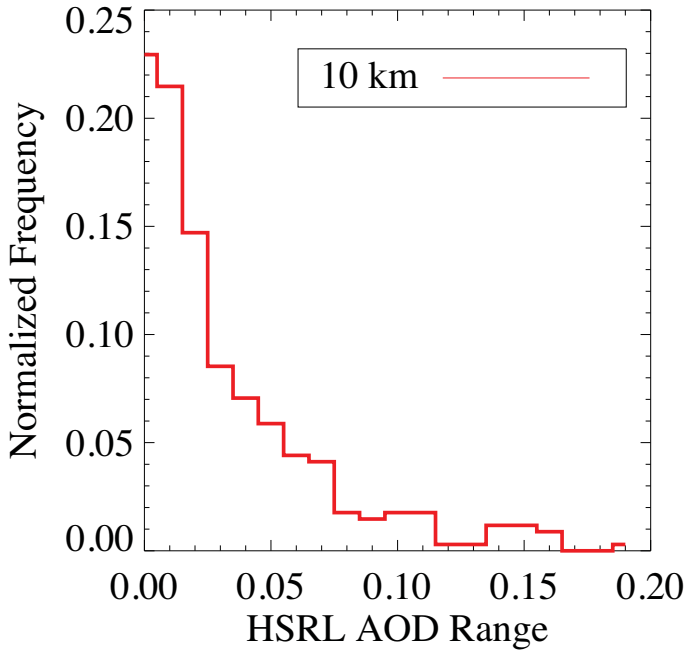

Fig. 5. The maximum difference between HSRL 0.55 µm AOD measurements observed within a MODIS 10 km pixel, normalized by the total frequency. Only MODIS pixels that contain 6 or more HSRL measurements are included.

AMTD
6, 1683–1716, 2013

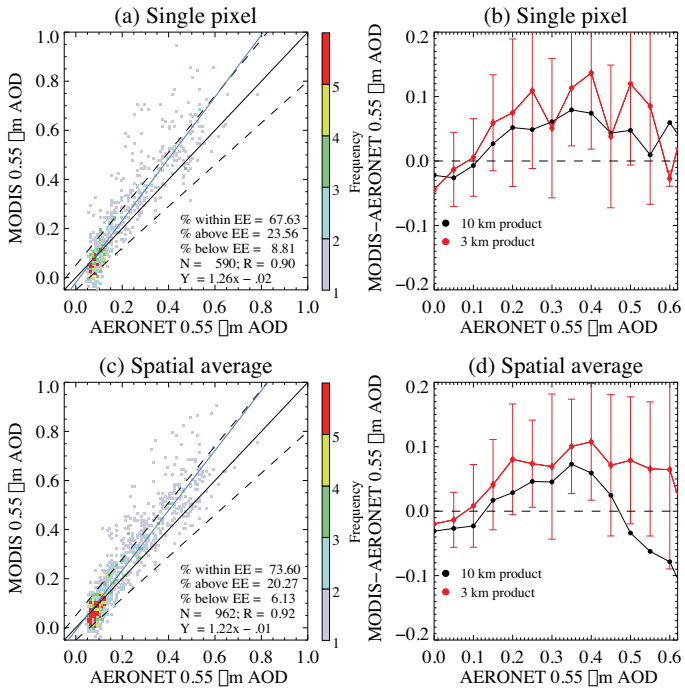

Fig. 6. (a) Density scatterplot of MODIS/SP collocations for AOD at 0.55 µm, using the single pixel collocation technique. Expected error over land (±0.05 + 0.15 AOD) is shown in the dashed lines, the best fit line is shown by the solid blue line, and the one-to-one line is shown in the solid black line. **(b)** Average difference between MODIS single pixel collocations and SP 0.55 µm AOD, as a function of SP 0.55 µm AOD. ±1 standard deviation is shown for the 3 km product. **(c)** As in **(a)**, but the MODIS 5 × 5 pixel spatial average collocation is used. **(d)** As in **(b)**, but the MODIS 5x5 spatial average collocation used.

AMTD
6, 1683–1716, 2013

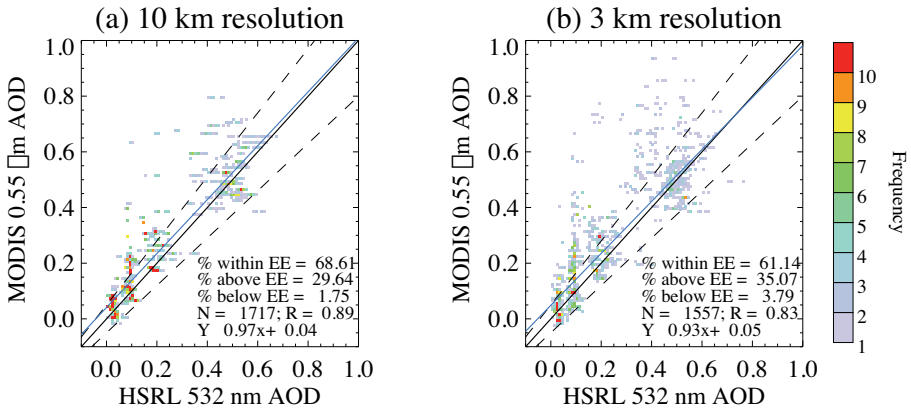

Fig. 7. Density scatterplot of MODIS/HSRL collocations for AOD at 0.55 µm for MODIS and 532 nm for HSRL for the 10 km MODIS product **(a)** and the 3 km MODIS product **(b)**. The MODIS AOD is sampled along the HSRL flight path; no spatial or temporal averaging is performed. Expected error over land (±0.05 + 0.15 AOD) is shown in the dashed lines, the best fit line is shown by the solid blue line, and the one-to-one line is shown in the solid black line.

AMTD
6, 1683–1716, 2013

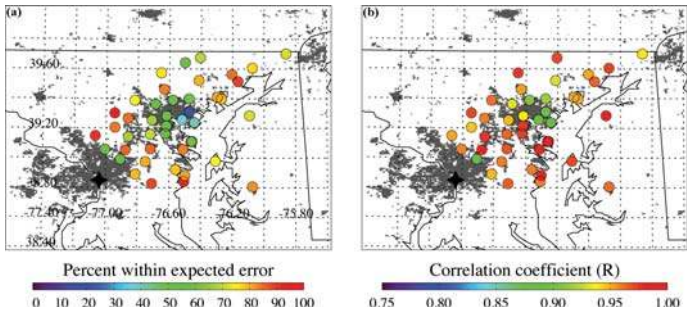

Fig. 8. (a) Percent of 3 km spatially averaged MODIS/SP collocations of 0.55 µm AOD within expected error (±0.05 + 0.15 AOD) at each SP station. **(b)** Correlation coefficient between 3 km spatially averaged MODIS 0.55 µm AOD and SP temporally averaged 0.55 µm measurements at each station. Land identified as urban/built up by the MODIS land cover product (MCD12Q1) is plotted in grey in both panels.

AMTD
6, 1683–1716, 2013

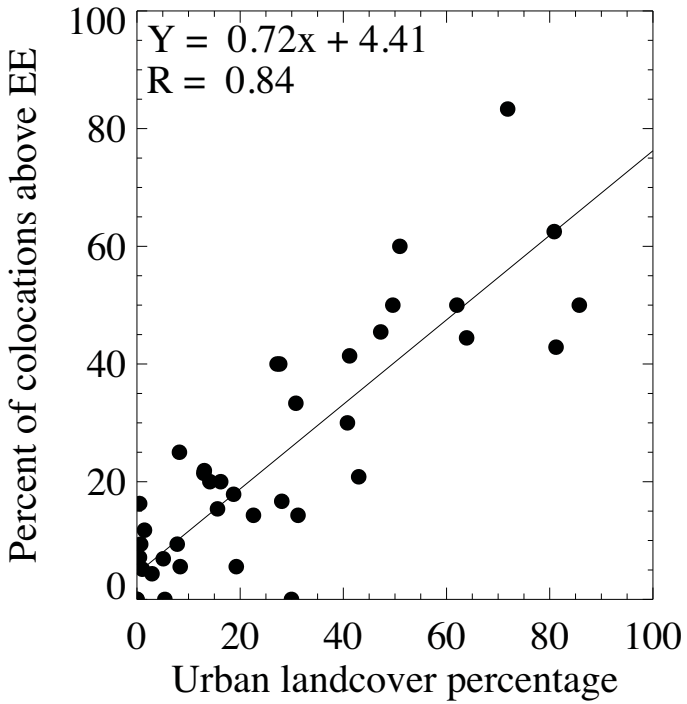

Fig. 9. Percent of 3 km spatially averaged MODIS/SP 0.55 µm AOD collocations above expected error (+0.05 + 0.15 AOD) at each SP station, plotted against the percentage of pixels within the 15 km by 15 km collocation box identified as urban by the MODIS land cover product.

AMTD
6, 1683–1716, 2013

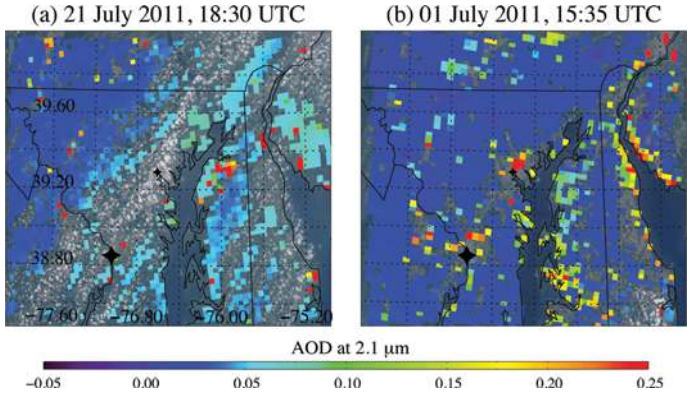

Fig. 10. (a) 3 km AOD at 2.1 µm observed by MODIS-Aqua on 21 July 2011 at 18:30 UTC. **(b)** 3 km AOD at 2.1 µm observed by MODIS-Terra on 1 July 2011 at 15:35 UTC. Only land pixels with a QA = 3 are shown. Washington D.C. is shown with the large black star and Baltimore is shown with the small black star. The true color image, created from the MODIS red, green and blue bands, is shown in the background.

AMTD
6, 1683–1716, 2013